Flexible bio-composites with continuous natural fibre and bamboo charcoal: enhanced flame retardancy, mechanical resilience, energy-absorbing & printability performance

Kaveh Rahmani , Callum Branfoot , Sarah Karmel , Kevin Lindsey & Mahdi Bodaghi

Taylor & Francis
Taylor & Francis Group

Flexible bio-composites with continuous natural fibre and bamboo charcoal: enhanced flame retardancy, mechanical resilience, energy-absorbing & printability performance

Kaveh Rahmani[a], Callum Branfoot[b], Sarah Karmel[c], Kevin Lindsey[d] and Mahdi Bodaghi [a]

[a]Department of Engineering, School of Science and Technology, Nottingham Trent University, Nottingham, UK; [b]Engineering Operations, National Composites Centre, Bristol, UK; [c]Rheon Labs, London, UK; [d]Far-UK Ltd., Nottingham, UK

ABSTRACT

This study presents a novel sustainable flexible bio-composite reinforced with bamboo charcoal (BC) and continuous flax fibres (CFF), designed to achieve exceptional thermo-mechanical features. Unlike conventional 3D-printed composites that rely on synthetic reinforcements, this research pioneers the synergistic integration of BC and CFF within a bio-based thermoplastic polyurethane (TPU) matrix using dual-feed 3D printing. BC/CFF incorporation enhances interfacial adhesion, as evidenced by scanning electron microscopy, leading to superior load transfer efficiency. Dynamic mechanical analysis confirms a substantial increase in storage modulus, improving structural stiffness, while melt flow index assessments demonstrate retained extrudability/printability. The addition of 3 wt.% BC and CFF achieves a 1571% increase in tensile strength relative to pure TPU. Furthermore, flame retardancy is significantly improved, with a 52% reduction in burning rate, achieving a UL-94 V-1 rating and a limiting oxygen index of 29.5% vol. Cyclic tensile tests reveal hyper-visco-pseudo-elastic behaviour, stress softening, and high energy-dissipation capacity, confirming suitability for dynamic applications. Meta-bio-composites with quasi-zero stiffness, force regulation, and superior energy absorption/dissipation exhibit a 933% improvement in specific energy absorption, making them ideal for protective applications. These findings establish bio-composites and their meta-structures as high-performance, sustainable alternatives to synthetic counterparts, unlocking new possibilities for automotive/logistics/furniture, and safety-critical applications.

1. Introduction

With increasing demand for sustainable, high-performance materials in industries such as automotive, construction, aerospace, and medical/sport/safety gears, composite Additive Manufacturing (AM), or 3D printing, has emerged as a pivotal technique, especially for thermoplastics that offer recyclability and customisability. One particularly noteworthy AM process is the fused filament fabrication (FFF) method, which has been successfully developed for 3D printing both pure thermoplastics and composites reinforced with common inorganic or synthetic fibres. FFF holds immense potential for various sectors, offering structural advantages over traditional materials [1,2]. Continuous fibre-reinforced composites traditionally rely on glass, carbon, or aramid fibres, but growing environmental concerns have shifted focus towards bio-based

composites using natural fibres (NF) [3,4]. In recent decades, sustainability concerns, regulatory pressures, and surrounding legislation have driven industries to seek alternatives to petroleum-based materials to make renewable products [5]. Therefore, NFs are gaining attention as sustainable alternatives due to their biodegradability and lower environmental impact during production and use [6,7]. In this respect, NFs have been employed to mostly reinforce rigid polymers and make green products. NFs such as hemp, flax, jute, sisal, and bamboo have shown advantages over common inorganic or synthetic fibres [8,9]. Integrating NFs into 3D printing further enhances sustainability by reducing greenhouse gas emissions and pollution associated with synthetic fibres [10]. Natural fibre-reinforced composites offer high strength, safety, and environmental benefits, making them suitable for eco-

friendly applications. Recent studies have emphasised their promising mechanical properties, driving interest in their development. The current research highlights the potential of NFs to replace synthetic fillers and/or reinforcements in advanced composites, aligning with global sustainable development goals [11,12].

While rigid fibre-reinforced AM composites have enabled high stiffness and strength, emerging applications in soft robotics, wearable protection, and energy-absorbing devices require flexible and multifunctional materials, driving interest in elastomeric matrices [13,14]. Elastomer-based composites exhibit exceptional energy absorption, ultra-stretchability, and resilience, making them ideal for applications such as soft robotics, wearable devices, seals, and vibration isolators, which can not be addressed using traditional rigid composite materials [15]. Their visco-elastic behaviour, along with their sensitivity to time, temperature, and strain rate, provides a high level of tunability and adaptability [16]. Among elastomeric materials, thermoplastic polyurethanes (TPU) stand out as one of the most widely used materials due to excellent flexibility, elasticity, and durability, making this polymer class a popular choice for applications in automotive, construction, aerospace, and medical sectors [17]. While conventional TPUs are fully recyclable, some bio-based alternatives are also biodegradable and environmentally friendly, making it a preferred alternative to similar polymer classes [18]. Recently, the mechanical performance of 3D printed TPU has been improved through fibre reinforcements. This can enhance mechanical properties, provide a balance of between strength and flexibility via superior load transfer efficiency, and increase toughness. For example, Pechlivani et al. [19] explored mechanical properties and energy absorption capabilities of 3D-printed TPU reinforced with continuous carbon fibres (CCFs) using a filament co-extrusion technique. They found that the composites show enhanced flexural performance and improved mechanical response, making them suitable for impact absorption applications. Hao et al. [20] investigated how varying 3D printing parameters affect the mechanical properties of TPU reinforced with CCFs. They demonstrated that lower layer thickness and optimised printing speed enhance tensile yield strength and flexural modulus. Through the above-mentioned explorations, TPU 3D printing reinforced by continuous synthetic fibres could offer exceptional strength-to-weight ratio and thermal stability, while continuous NFs are yet to be explored as a sustainable 3D printable alternative with eco-friendly benefits and high performance. NFs can offer a unique combination of attractive features, such as strength, lightweightness, bio-degradability, cost-effectiveness, and thermal and acoustic insulations. Flax fibres

are one of the most promising lignocellulosic NFs. They show remarkable specific mechanical properties comparable to synthetic fibres, making them widely adopted in the automotive and construction sectors [21]. Short flax fibres have been successfully used to reinforced TPU. For example, Tayfun et al. [22,23] reinforced a bio-based TPU matrix with short flax fibres and produced the biocomposite via melt compounding for injection moulding. The bio-composites showed improved mechanical properties like tensile strength, Young's modulus, and storage modulus, and water absorption. Ansaripour et al. [24] reinforced the polylactic acid (PLA) (70%)-TPU(15%) hybrid matrix with 15% short flax fibres for 3D printing. The composite showed a remarkable 120% enhancement in impact strength compared to neat PLA.

In many industrial sectors like automotive, aerospace, transportation, construction, and furniture, the demand for flame-retardant materials has increased due to stringent safety regulations and fire performance requirements. However, conventional flame-retardant additives, such as halogenated and phosphorus-based compounds, have been banned in regions like the EU since 2021 due to their environmental and health risks. These additives not only raise ecological concerns but may also compromise mechanical properties, highlighting an urgent need for more sustainable and environmentally friendly alternatives [25,26]. Bamboo has been recognised as one of the best options for producing safe and sustainable composite materials due to its abundance, rapid growth rate, desirable mechanical strength, and environmental compatibility [27,28]. In addition to these properties, using bamboo reinforcement charcoal (BC) can enhance the flame retardancy of base materials like TPU. Wu et al. [29] used powder bamboo fibres as charring agent to create flame-retardant TPU composites via extrusion and cold press. The composites achieved a 30.5% limiting oxygen index (LOI) and V-0 rating, with a peak heat release rate (pHRR) of 190 kW/m^2, 86.0% lower than neat TPU, making them strong candidates for use in firesafe consumer and industrial products.

Despite the recent progress in 3D-printed composites, the integration of continuous natural fibres like continuous flax fibres (CFF) with elastomeric matrices such as TPU for structural and flame-retardant applications remains unexplored. Previous studies have primarily reinforced TPU with short natural fibres or synthetic reinforcements such as carbon/glass fibres to enhance mechanical properties, but their impact on flame retardancy and energy absorption has shown limited effect [30,31]. Moreover, while BC has shown promise as a natural flame retardant, its synergistic effect with CFF in 3D-printed TPU composites remains unexplored. The key challenge lies in balancing

mechanical strength, flexibility, and flame retardancy while maintaining optimal printability, a gap that this study aims to address.

This research introduces a novel, 3D-printable bio-composite combining CFF and BC reinforcement within a TPU matrix, offering enhanced thermo-mechanical performance under various loading histories and strain rates. Figure 1 presents an overview of the development process for TPU-based bio-composites reinforced with BC and CFF, from material preparation and extrusion to 3D printing and potential applications. The newly developed materials were characterised through comprehensive monotonic and cyclic loadings at various strain rates, as well as flammability testing, to provide a library of material prototypes with a focus on non-linearity, visco-elasticity, stress softening (Mullins effect), residual strain, and recoverability/reusability. Furthermore, the developed bio-composites were 3D-printed into meta-bio-composites, exhibiting constant force response, quasi-zero stiffness, and energy absorption/dissipation.

The proposed bio-composite would be suitable for many applications such as flame-retardant protective packaging, fire-retardant spacers, fire fighter gloves, duty boots and hoses, wires/cables, pipes, footwear, automotive bellows, mounts and seals, furniture cushions, and electrical insulators. These findings are expected to be instrumental in supporting responsible and sustainable manufacturing, as well as circular economy principles.

2. Bio-composite materials, manufacturing and testing

2.1. Matrix material

In this research, bio-based TPU 93 A pellets (Nanovia, France) were used as the matrix material (Figure 2). Bio-based TPU from renewable resources is known for being biodegradable, recyclable, environmentally friendly, and moisture resistant [32]. Also, TPU is a versatile elastomeric polymer known for its excellent

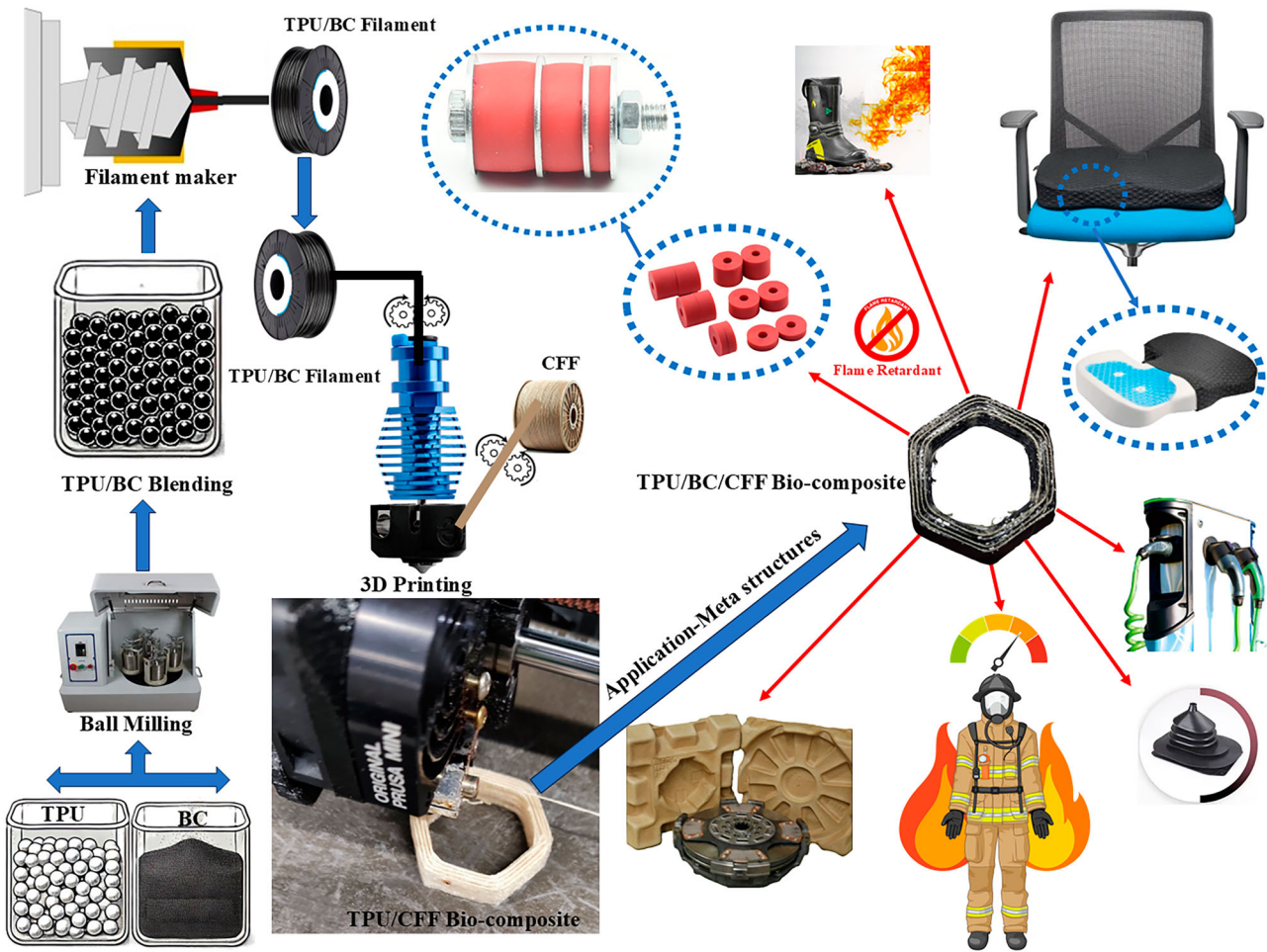**Figure 1.** A schematic illustration of TPU/BC/CFF bio-composite production, from material preparation and extrusion to FFF 3D printing of meta-structures. Potential applications include flame-retardant protective packaging, fire-retardant spacers, firefighter gloves, helmets, duty boots and hoses, wires/cables, pipes, automotive bellows, mounts and seals, furniture cushions, and electrical insulators.
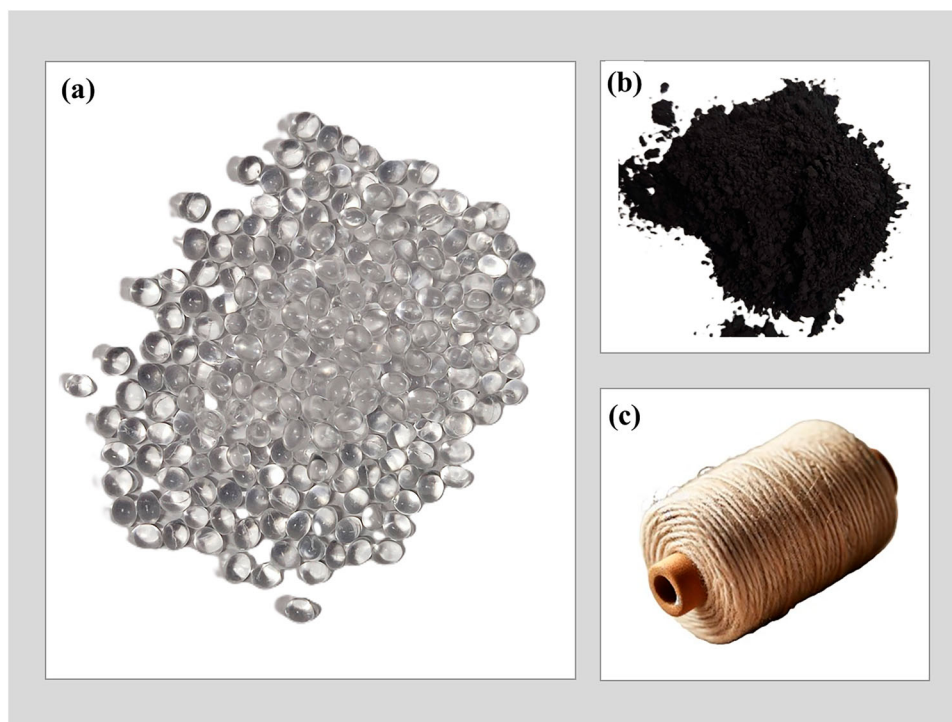
Figure 2. Bio-composite elements: (a) TPU pellets, (b) BC powder, (c) CFF.

flexibility, high elongation at break, abrasion resistance, and good mechanical strength. It exhibits hyper-elastic behaviours, allowing large reversible deformations, making it ideal for applications involving dynamic loading, damping and shape recovery [33].

2.2. Reinforcement (powder and fibre)

BC powder with particle size of approximately 25 µm from a natural plant resource was provided as a raw particle-reinforcement material by Takesumi Ltd. (Japan). It offers functional benefits such as flame retardancy, moisture regulation, electrical conductivity, and potential improvement in stiffness and damping when used as a filler in polymer composites. Despite their advantages, thermoplastics often exhibit suboptimal mechanical properties. To address this limitation, natural continuous fibre reinforcements were employed to enhance the mechanical attributes of the printed products. In this study, CFF, another natural plant resource, was supplied by Bobbin Lace Linen Threads and used as reinforcement to improve structural strength [34]. The average diameter of the flax fibres was approximately 300 µm, and they were subjected to an alkali surface treatment using 5 wt.% NaOH solution for 1 h to improve interfacial bonding with the TPU matrix. This treatment helps to remove surface impurities and enhance the fibre-matrix adhesion. In addition, the selected flax yarn, a bundle of fine unwaxed natural

linen fibres, has a linear density of 38 Tex × 2 2-ply thread.

2.3. Extrusion process for filament making and 3D printing

The process begins with raw materials, namely TPU pellets and BC particles, and involves ball milling, composite filament extrusion, and 3D printing of TPU/BC bio-composite filaments reinforced by CFF, as depicted in Figure 3. It also showcases the 3D-printed TPU, TPU/BC and TPU/BC/CCF samples. The details of each step are elaborated below.

2.3.1. Drying process and ball milling of composites

In the first stage, the TPU raw pellets were dried in an oven at 60°C for 6 h. To create TPU composites with varying BC content (0, 3, and 5 wt.%), the dried pellets were placed in a planetary ball mill mixer at an operating frequency of 30 Hz. It uses 12 hard chromium steel balls with a 10 mm diameter and 5 same metal balls with a 15 mm diameter and has a ball-to-powder mass ratio of 1:2 in a steel vial with a volume of 150 ml. Composites were milled and blended at a rotational speed of 100 rev/min for 10 min to ensure a homogeneous distribution of BC particles within the TPU pellets. The selection of 3 and 5 wt.% BC was based on a combination of trial-and-error and previous work [34].
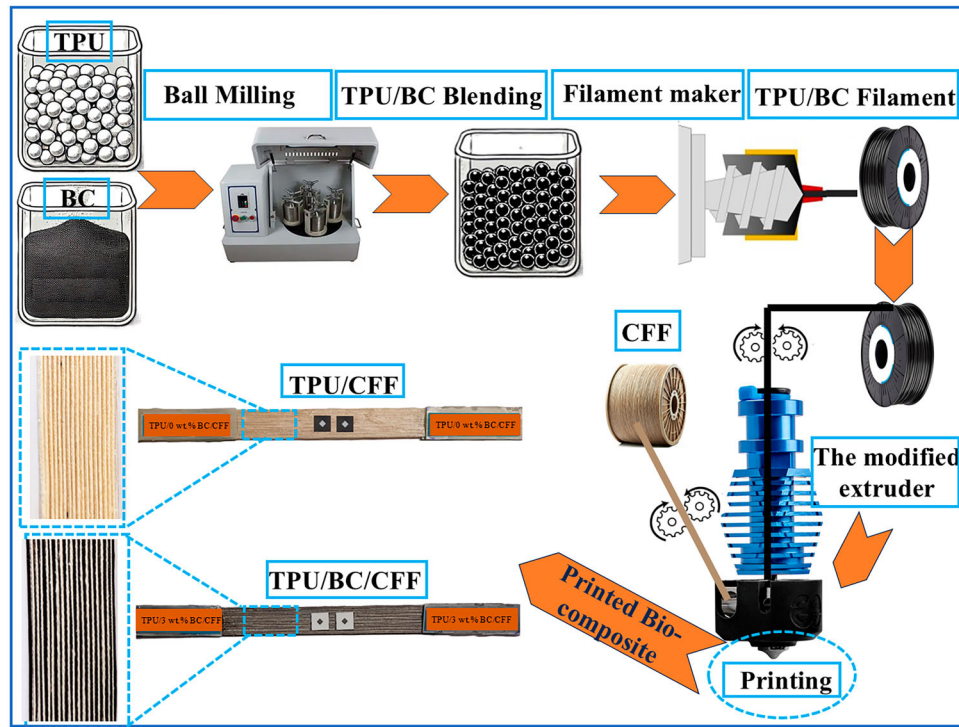
Figure 3. A detailed schematic of the development of bio-composites from preparation to fabrication involving: mixing raw TPU and BC particles, filament extrusion, and 3D printing of continuous natural fibre-reinforced TPU/BC composites to create testing samples.

2.3.2. Composite filament extrusion

The TPU/BC composite mixtures were then extruded using a single-screw extruder (3DEVO, the Netherlands) to produce filaments with a diameter of 1.75 mm, which were utilised for 3D printing all samples. Table 1a outlines the extrusion parameters applied for the TPU/BC bio-composite filaments.

2.3.3. 3d printing process and simultaneous feeding of CFF

A custom-designed extruder along with a single-nozzle FFF 3D printer (Original Prusa MINI+) was employed. The printer, equipped with a nozzle diameter of 1.8 mm and set to a temperature of 235°C, was used to simultaneously feed both the TPU/BC bio-composite filament and the CFF, enabling the development of polymer composites reinforced with CFF.

Figure 3 provides a detailed schematic of producing filament TPU/BC composite and illustrates how the TPU/BC bio-composite and CFF are fed into the modified extruder through two distinct channels before being merged and extruded through a single-output nozzle. All samples were 3D printed using consistent printing parameters, as outlined in Table 1b. TPU filaments and samples reinforced with different BC percentages are labelled as TPU/X(= 0, 3, 5) wt.% BC.

Additionally, TPU/X wt.% BC samples reinforced with CFF are designated as TPU/X(= 0, 3, 5) wt.% BC/CFF.

2.4. Composite characterisations at micro- and macro-scales

2.4.1. Scanning electron microscopy (SEM)

Scanning electron microscopy (SEM, JSM-7100 F LV FEG) was used to carry out a microstructural analysis to assess the BC distribution, CFF distribution and the fracture

Table 1. Fabrication parameters for extruding TPU/BC filament (a) and 3D printing (b).

Parameters	Value
(a)	
Extrusion temperature at heat zone 1 (°C)	200
Extrusion temperature at heat zone 2 (°C)	235
Extrusion temperature at heat zone 3 (°C)	215
Extrusion temperature at heat zone 4 (°C)	195
Die temperature (°C)	185
Fan speed (m/s)	100
Extrusion rotation speed (rpm)	3.5
Filament diameter (mm)	1.75
(b)	
Nozzle diameter (mm)	1.8
Layer thickness (mm)	0.2
Printing speed (mm/s)	35
Infill density (%)	100
Printing pattern	Linear
Nozzle temperature (°C)	235
Bed temperature (°C)	65

surfaces to understand the bonding between TPU, BC, and CFF. Prior to imaging, the samples were coated with a thin layer of gold to enhance the image clarity.

2.4.2. Dynamic mechanical thermal analysis (DMTA)

A DMTA was conducted to investigate the thermo-mechanical behaviours of TUP composites. The study examined the effects of natural fibres and BC particles on storage modulus and glass transition temperature (T_g), while also identifying the thermal zones of pure TPU and its composites. Tests were performed using a DMTA machine (DMA 8000, PerkinElmer) across a temperature range of $-100°C$ to $+100°C$, with a heating rate of 5°C/min and a frequency of 1 Hz. Samples were tested in the bending mode using a cantilever beam with dimensions of 30 mm length, 8 mm width, and 1 mm thickness, following the ASTM D4065-01 standard.

2.4.3. Melt flow index (MFI)

The MFI of TPU and TPU/BC bio-composites was measured using a melt flow index machine at 210°C and a load of 5 kg, in accordance with ISO 1133. Five samples were tested, and the results were averaged.

2.4.4. Underwriters' laboratories (UL-94)

The flammability properties of the bio-composites were analysed using a combination of UL-94 horizontal and vertical burning tests, LOI measurements, and cone calorimeter tests (CCTs). The methodologies used are described as follows:

2.4.4.1. The flammability was assessed in accordance with ASTM D635-22 to measure the burning rate and duration in a horizontal position [35]. The prepared samples had the following measurements: 125 mm length, 13 mm width, and 3 mm thickness. Horizontally mounted printed samples were placed in a fume hood and marked at 25 and 100 mm from one end.

2.4.4.2. To classify materials based on their flame-extinguishing ability and resistance to dripping during combustion, vertical burning tests were also conducted using a UL-94 vertical flame chamber instrument, following ASTM D3801, samples with dimensions of 125 mm length, 13 mm width, and 3 mm thickness. The LOI values, which indicate the minimum oxygen concentration required to sustain combustion, were measured using an oxygen index metre in compliance with ASTM D2863. This analysis offers crucial insights into the flame-retardant properties of the composite materials.

2.4.4.3. To assess combustion behaviour and heat release characteristics, CCTs were performed in line with the ISO 5660 standard. These tests yielded a detailed dataset on key parameters such as heat release rate, total heat released, and time to ignition (TTI), offering a comprehensive understanding of the flame-retardancy performance of the composites under realistic fire conditions.

2.4.5. Mechanical behaviour

The following tests were carried out to characterise and understand the mechanical behaviour of pure TPU and TPU bio-composites:

2.4.5.1. Monotonic tensile test. The tensile tests for pure TPU, TPU/BC, TPU/CFF and TPU/BC/CFF samples were performed at three different speeds: 5, 10 and 50 mm/min to investigate the rate-dependent and visco-elastic behaviours of the materials as dictated by ASTM D638 and D3039. A Shimadzu AG-X plus machine were used for these tests. The TPU and TPU/BC samples were stretched up to 200% strain of the gauge length, while TPR/CFF and TPU/BC/CFF samples were stretched to break.

2.4.5.2. Cyclic tensile tests. To evaluate the stress softening (Mullins effect) and stress reduction due to hysteretic/visco-elastic behaviour in the pure TPU and TPU reinforced with BC and CFF, uniaxial cyclic tension tests were conducted at a speed of 5 mm/min. The tests involved three cycles with engineering strains of 50, 100, and 150%. Initially, a preload of 0.1 N was applied to the virgin samples. During the first step, the samples underwent three loading cycles at 5 mm/min, with the maximum strain raising incrementally by 50% in each cycle. After reaching the target strain in each cycle, the samples were unloaded back to the zero-offset condition. The final cycle reached a maximum engineering strain of 150%, which was determined based on prior monotonic tests. Unloading was programmed as complete when the force became zero.

Figure 4 illustrates images of the printed samples designed according to ASTM standard along with the testing method adhering to ASTM standard, and finally close-up images of the fibres within the composite samples.

To measure the axial strain, two-gauge marks spaced 10 mm apart were placed on the gauging section of each specimen as shown in Figure S1 in the supplementary material. The change in distance between these marks was continuously monitored on-line by camera. Throughout the test, the engineering strain was controlled during both loading and unloading based on the measured distance. Since the machine speed (v) used in the experiments does not directly represent the strain rate (e) the following relationship was
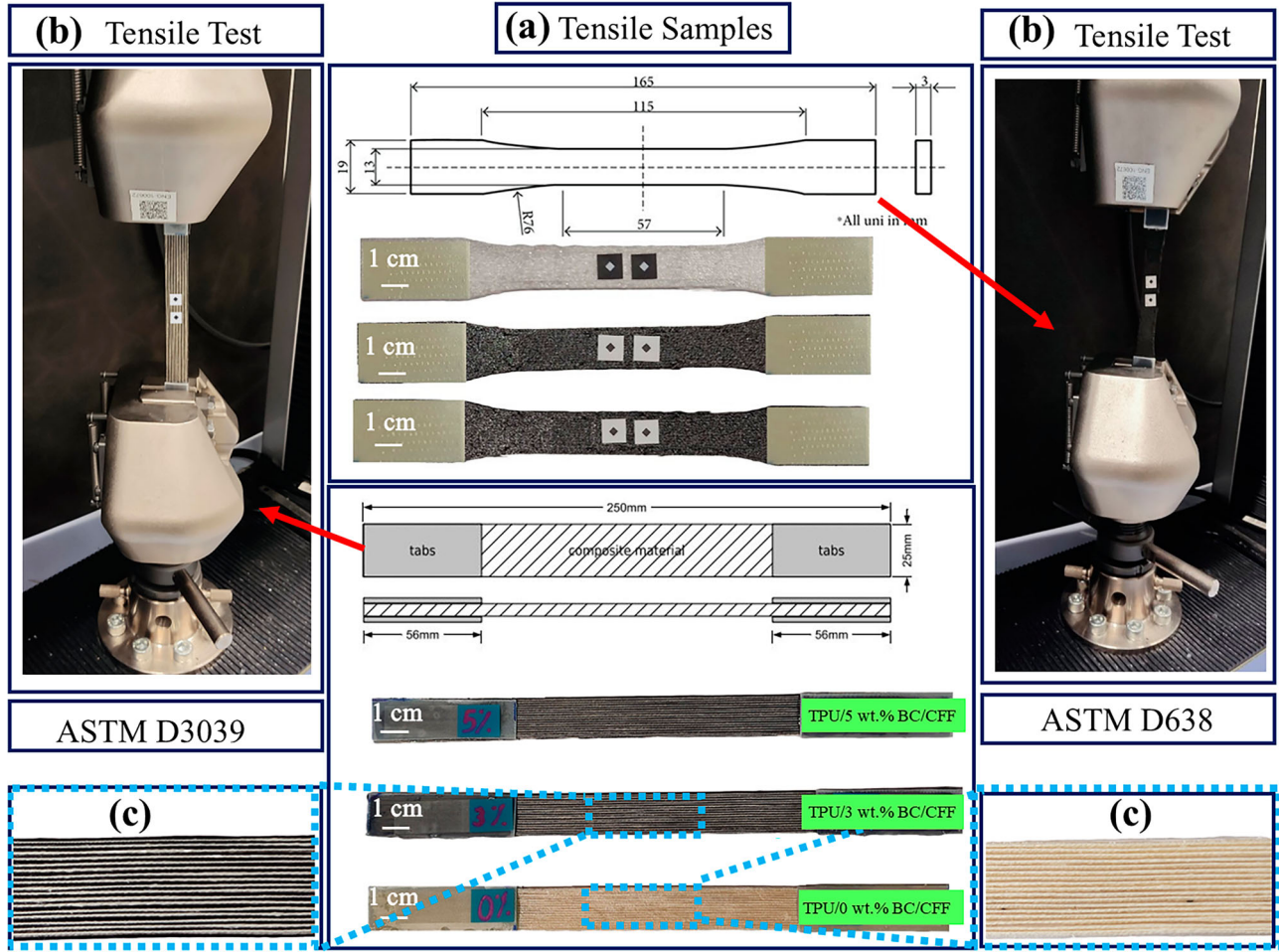
Figure 4. (a) Samples designed according to ASTM standard, (b) images of the printed testing samples adhering to ASTM standard, and (c) close-up images of the fibres within the samples.

established for it:

$$\dot{e} = \frac{v}{60 L_O} \qquad (1)$$

Here, L_0 represents the initial distance between the two-gauge marks in millimetres, and v denotes the machine's speed in millimetres per minute. Table 2 lists the corresponding strain rates for each speed. All tests were conducted under ambient laboratory conditions without conditioning, with each group tested at least five times to ensure repeatability. The average values were reported for each group. To maximise strength, all samples were 3D printed in the longitudinal direction.

Table 2. The strain rate for different testing speeds.

Speed [mm/min]	Strain rate [1/s]
5	0.008
10	0.016
50	0.083

3. Results and discussion

3.1. Microstructure study

This section investigates SEM micrographs and further determines the volume fraction of CFF yarns in the developed TPU-based bio-composites.

Figure 5 presents SEM images of the microstructure of cross section and flat surfaces of TPU/BC/CFF tensile specimens. SEM original images are provided in the supplementary material (Figure S2) to support this observation. The SEM of cross section images presented in Figures 5a and b reveals that 3 wt.% BC powders have homogeneous dispersion within the TPU matrix. It is seen that excessive addition of BC reinforcements (from 3 wt.% to 5 wt.%) can lead to particle agglomeration and porosity, resulting in non-uniform dispersion and less uniform distribution within the matrix. This reduced dispersion quality at higher loading levels (i.e. 5 wt.%) is likely due to the intrinsic tendency of the BC particles to interact with each other rather than with the TPU matrix. This self-affinity can lead to
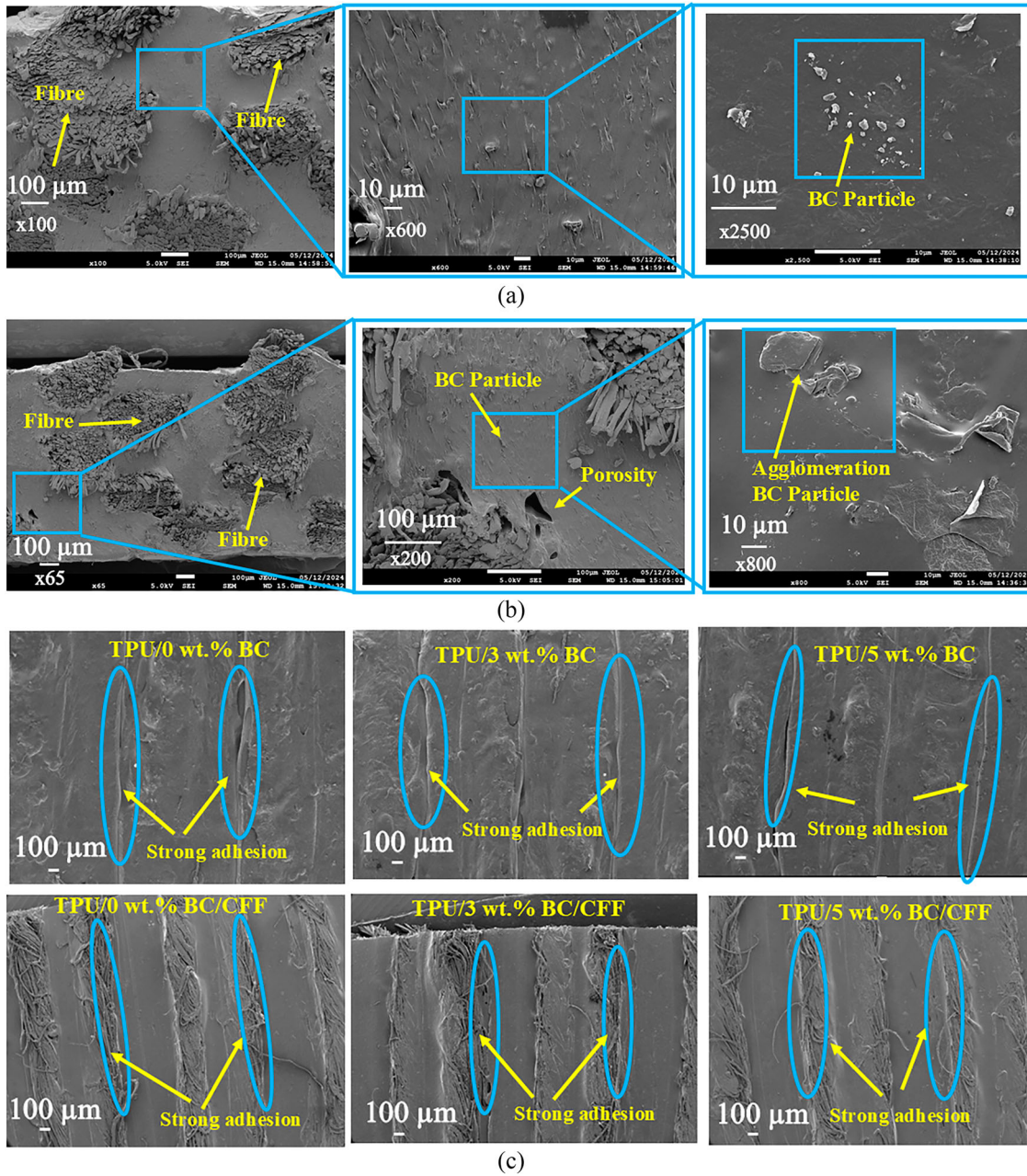
Figure 5. SEM microphotograph of crosse section (a) TPU/3 wt.% BC/CFF and (b) TPU/5 wt.% BC/CFF bio-composite, showing bonding between CFF, BC and TPU matrix in SEM microphotograph of flat surfaces (c).

agglomeration when the filler concentration exceeds a certain threshold, thereby reducing uniform distribution [34]. As a result, at lower concentrations (such as 3 wt.%), better dispersion is observed due to fewer particle-particle interactions.

As can be seen in the flat surfaces of the specimens in Figure 5c, the fibre–matrix interface exhibits strong adhesion, which is critical for the mechanical performance of fibre-reinforced polymer composites. This strong bonding arises from both chemical and mechanical interlocking and coupling among the TPU matrix, BC particles, and continuous flax fibres (CFF). The BC particles are uniformly distributed and enhance surface roughness, improving compatibility with the TPU matrix. Such interfacial characteristics promote efficient stress transfer and load distribution during mechanical loading. Moreover, CFFs are visible at the interface, contribute to crack-stopping mechanisms. These behaviours may lead to the improved strength observed in TPU and TPU/BC biocomposites upon CFF incorporation.

Figure 6 also displays SEM images of the microstructure of the fracture surfaces of TPU/BC/CFF specimens. SEM original images are provided in the supplementary material (Figure S3) to support this observation. The
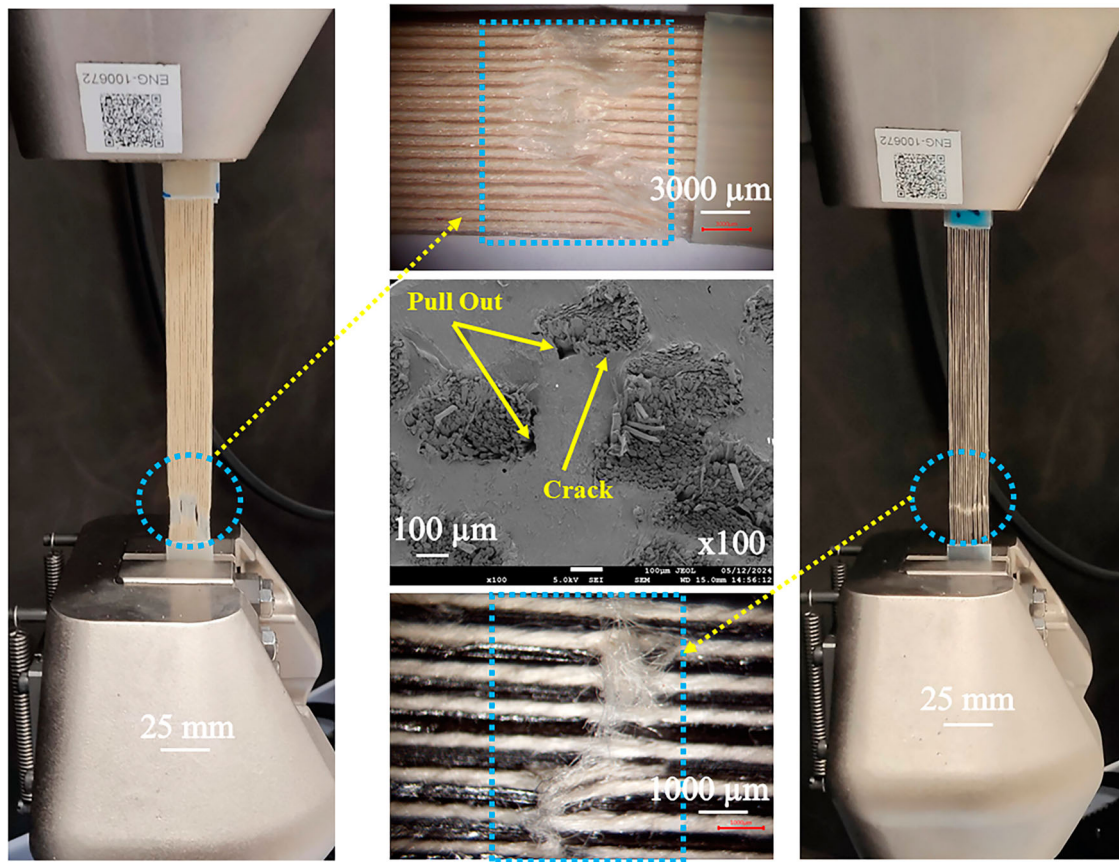
Figure 6. SEM image of the microstructure of the fracture surfaces of TPU/BC/CFF tensile specimen.

observed fracture and damage mechanisms include matrix fracture, fibre breakage, and fibril pull-out from the flax fibres, resulting from the applied tensile stress. These failure mechanisms are primarily controlled by interfacial debonding, crack propagation, and matrix yielding. Stress concentrations at the fibre–matrix and particle–matrix interfaces initiate debonding, which serves as a precursor to micro-crack formation. As loading continues, these cracks propagate through the TPU matrix and along weakened interfacial regions [36]. Additionally, signs of fibre pull-out and matrix shear deformation are evident, contributing to energy dissipation and improved fracture toughness [37]. This combination of interfacial separation, matrix damage, and progressive crack growth is consistent with failure patterns typically reported in natural fibre-reinforced polymer composites [38]. Accurately determining the CFF volume fraction is important for the development of printed composites and serves as a fundamental indicator of composite quality, impacting its mechanical properties and performance. To measure the volume fraction of CFF in the TPU bio-composite, ImageJ software was utilised. A cross-section of an as-printed TPU bio-composite sample was prepared, and SEM images

of the cross-section were captured. These images were analysed using ImageJ software, as illustrated in Figure 7, to estimate the CFF volume fraction. SEM original images are provided in the supplementary material (Figure S4) to support this observation. The average CFF volume fractions were approximately 45%, 43%, and 40% for TPU/0 wt.% BC/CFF, TPU/3 wt.% BC/CFF, and TPU/5 wt.% BC/CFF, respectively.

3.2. DMTA

The storage modulus and tan δ are key parameters used to evaluate mechanical and visco-elastic properties of materials. DMTA was conducted to study the impact of incorporating CFF and BC particles on the storage modulus and tan δ of TPU. Figures 8a and b illustrate the storage modulus and tan δ values for pure TPU as the raw material and TPU reinforced with BC and CFF, respectively. From the curves in Figure 8, distinct visco-elastic states of the samples can be identified. These include the glassy state at low temperatures and a broad glass transition region between ∼ −50 and 50°C. Figure 8a reveals that the storage modulus value rises with the addition of BC and CFF reinforcement
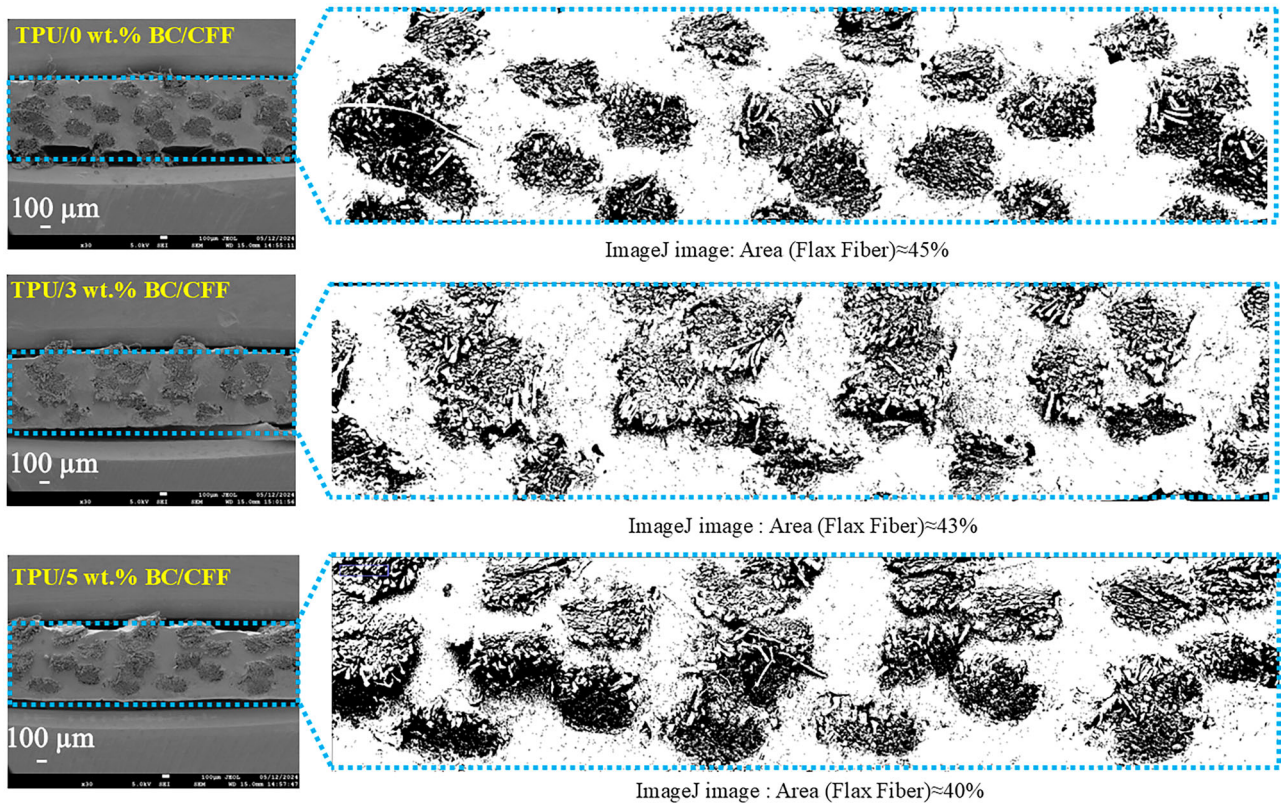
Figure 7. SEM images of TPU/BC/CFF bio-composite to determine CFF volume fraction using ImageJ software.

compared to pure TPU, indicating enhanced elastic stiffness and load-bearing capacity within the composite. A similar result was reported by [39] that increasing seed reinforcement leads to a significant rise in the storage modulus, confirming improved stiffness and structural integrity of the composite. Simultaneously, the tan δ in Figure 8b also decreases, reflecting less viscous energy dissipation due to reduced interfacial motion and internal friction and enhanced interfacial adhesion between the matrix and the reinforcements. It also shows T_g, represented by the midpoint of the tan δ peak, as about 0°C for pure TPU. Regarding TPU/0 wt.% BC/CFF, TPU/3 wt.% BC/CFF, and TPU/5 wt.% BC/CFF, T_g values read approximately 7.16, 8.6, and 10.1°C, respectively. Additionally, the α-relaxation temperatures, which mark the onset of the glass transition
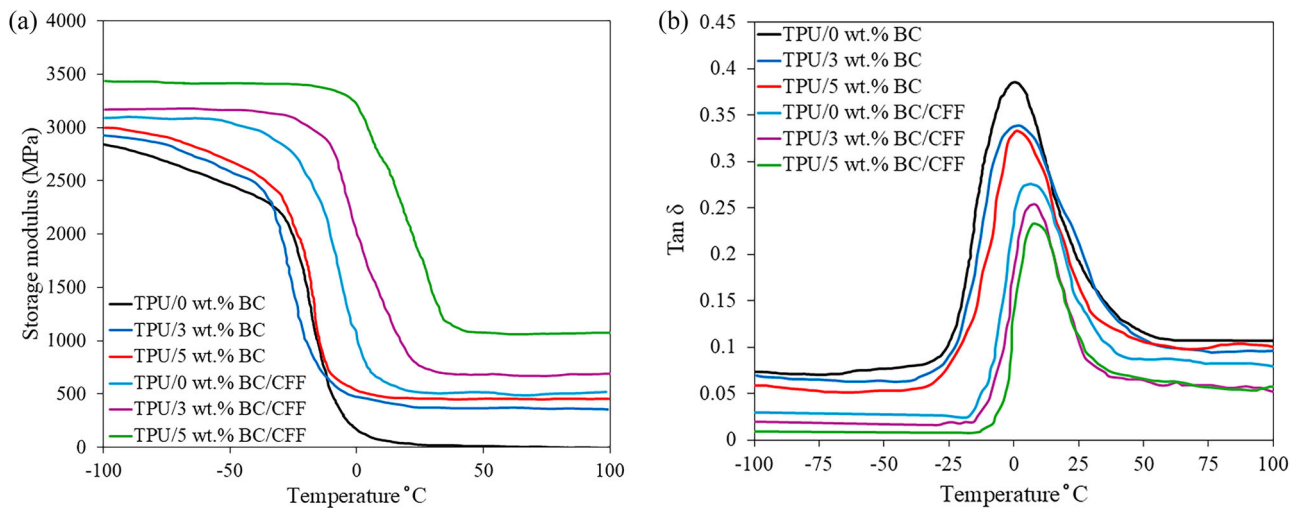

Figure 8. DMTA results of TPU and TPU bio-composites: (a) storage modulus, (b) tan δ.

region, along with the tan δ peak, were determined for the TPU/3 wt.% BC/CFF bio-composite. The α-relaxation temperature was found to be −23°C, while the tan δ peak occurred at 8.6°C. In this temperature range, long-range intermolecular movements of the polymer chains occur. The maximum amplitude of tan δ (damping factor) reaches 0.38 for pure TPU and drops to 0.23 for TPU/5 wt.% BC/CFF, limiting a bit damping properties.

3.3. MFI of TPU/BC bio-composites

The MFI of the developed bio-composites is discussed in this section to understand their extrudability feature. Table 3 presents the MFI values of TPU and TPU/BC. The MFI of pure TPU is 19.2 g/10 min. With the addition of 3 and 5 wt.% BC particles, the MFI of the TPU bio-composites decreases to 17.1 and 16.3 g/10 min, respectively. This reduction occurs because BC particles tend to favour interparticle interactions over adhesion to the TPU matrix. The agglomeration of BC particles within the matrix also increases melt viscosity, leading to lower MFI values [40]. Overall, it is found that the addition of BC has a minimal impact on the MFI value of TPU. It implies that processing challenges such as high shear mixing or feeding difficulties are unlikely to arise during extrusion filament making and 3D printing of TPU/BC bio-composites. Despite the slight reduction in MFI, the TPU/BC bio-composites possess an excellent level of extrudability and 3D printability and can still be effectively integrated with continuous fibres during 3D printing.

3.4. Flammability characteristics

The flammability characteristics of TPU and TPU bio-composites were assessed using UL-94 ratings, which involved horizontal and vertical burning tests, LOI, and CCTs (via TTI and pHRR). The findings are detailed in Table 4. Figure 9 also illustrates the appearance of the sample before and after horizontal/vertical burning tests, showing their post-burn conditions.

A key observation from Figure 9 is that the samples reinforced with CFF did not burn completely, while those without CFFs burned entirely. Initially, the bio-composite samples were subjected to the UL-94

horizontal burning test. Table 4 reveals that among the tested samples, TPU/5 wt.% BC/CFF, TPU/3 wt.% BC/CFF, and TPU/0 wt.% BC/CFF demonstrate the lowest burning rates, showing improvements of 52%, 47% and 37%, respectively, compared to the pure TPU. This reduction in burning rate can be attributed to several factors such as: (1) The presence of natural fibres and BC particles forms protective layers that hinder heat and volatile substances from penetrating the composite [34]. (2) The addition of BC and CFF enhances flame retardancy by reducing the material's overall flammability and dripping. (3) CFF improves the composite's structural integrity and aids in the formation of a protective layer, leading to lower burning rates and incomplete combustion compared to the pure TPU. In contrast, the pure TPU exhibits the highest burning rate, likely due to its rapid thermal degradation during combustion, making it more vulnerable to flames.

The flame retardancy of TPU and its bio-composites was further assessed using UL-94 vertical burning and LOI tests, results of which are presented in Table 4. The specimens were cut into standard dimensions and tested using an LOI apparatus in a controlled environment. The results are reported in volume percent (vol.%), which is the standard unit indicating the minimum oxygen concentration required to sustain combustion. The pure TPU possesses an LOI value of 19.5%. Adding BC slightly increases the LOI of TPU to 21%, while the simultaneous incorporation of CFF and BC results in higher LOI values. The most significant improvement is observed for the TPU/5 wt.% BC/CFF composite achieving an LOI value of 29.5%. This enhancement is attributed to the formation of a char layer by the reinforcements as a thermal barrier, slowing the transfer of oxygen. Also, this compact carbonaceous layer acts as a physical barrier that limits heat transfer to the underlying material, slows down the release of volatile gases, and effectively reduces flame propagation. As a result, the composite exhibits a noticeable increase in LOI values. This behaviour aligns with findings reported in the reference [41],

Table 3. The results of MFI measurements for the TPU/BC bio-composites.

Samples	Melt flow index (g/ 10 min)
TPU/0 wt.% BC	19.2 ± 0.3
TPU/3 wt.% BC	17.1 ± 0.2
TPU/5 wt.% BC	16.3 ± 0.5

Table 4. UL-94, LOI and CCT results for TPU and TPU bio-composite

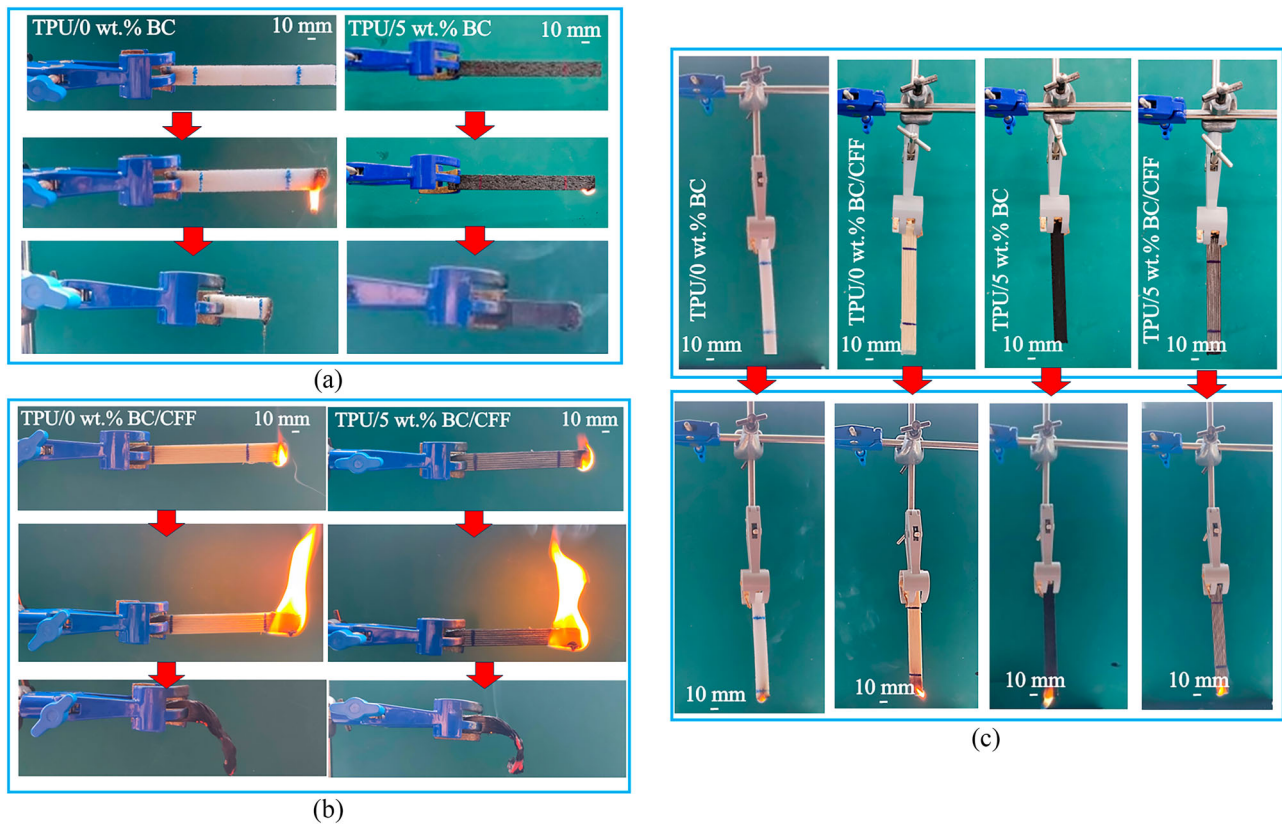| Samples	UL-94			LOI		
	Horizontal Burning rate (mm/min)	Vertical Dripping	Rating	(vol.%)	pHHR (kW/m²)	TTI (s)
TPU/0 wt.% BC	40	Yes	NC*	19.5	449	67
TPU/3 wt.% BC	32	Yes	NC	20.3	405	61
TPU/5 wt.% BC	29	Yes	NC	23.6	384	55
TPU/0 wt.% BC/CFF	25	Yes	V2	25.8	355	51
TPU/3 wt.% BC/CFF	21	Yes	V1	27.4	311	43
TPU/5 wt.% BC/CFF	19	Yes	V1	29.5	295	39

* No Classification (NC).

Figure 9. Visual documentation of clamping specimens and igniting by UL-94 rating for (a) TPU, TPU/BC and (b) TPU/BC/CFF, TPU/CFF composites under horizontal test; and (c) TPU, TPU/CFF, TPU/BC and TPU/BC/CFF composites under vertical test.

where the char layer formed during the combustion of natural fibre-reinforced composites has been shown to improve flame retardancy by promoting thermal insulation and reducing combustibility. In the UL-94 test, the rating of pure TPU improves from 'No Classification' (NC) to V1 with the addition of both BC and CFF.

The fire performance of the composites was further evaluated via cone calorimeter tests (i.e. CCTs). Key parameters such as pHRR and TTI were used to compare the fire behaviour of the composites as listed in Table 4. A reduction in HRR curves typically indicates an improved fire performance. The pHRR values for TPU/5 wt.% BC/CFF, TPU/3 wt.% BC/CFF and TPU/0 wt.% BC/CFF are 295 kW/m², 311 and 355 kW/m², respectively, representing a reduction of 34%, 30% and 21% compared to the pure TPU. Table 4 also implies a delay in the TTI with the incorporation of BC and CFF. This delay is attributed to the uniform dispersion of BC and the effective coating of CFF by TPU, promoting the formation of a protective char layer that acts as a barrier to heat transfer. This protective layer directly contributes to the observed reduction in pHRR values [41].

However, the addition of BC alone reduces the TTI of TPU, indicating earlier ignition compared to the pure TPU. This occurs because BC particles tend to act in the condensed phase during combustion that could decrease flammability properties. The earlier onset of thermal degradation in the TPU is due to the higher heat absorption caused by the BC. In contrast, the inclusion of CFF increases the total burning time compared to TPU with only BC. In this study, BC contributes to earlier degradation onset, it also improves flame retardancy by lowering the burning rate, as supported by calorimeter data. CFF, despite extending the burning time, helps improve structural integrity and reduce dripping.

The results presented in Table 4, Figures 8 and 9 along with the discussions highlight that incorporating BC particles and continuous CFF fibres into TPU not only enhances mechanical strength but also significantly improves the flame retardancy. They also reveal the potential of 3D-printed flame-retardant bio-composites reinforced with plant-based resources as sustainable and eco-friendly flexible materials for various applications like those illustrated in Figure 1. Such novel composite materials will enable the creation of a safer and sustainable product design paradigm promoting environmentally friendly practices.

3.5. Mechanical properties

3.5.1. Monotonic tensile tests

Monotonic uniaxial tensile tests were conducted at three speeds 5, 10, and 50 mm/min on the pure TPU and TPU bio-composite specimens.

Initial tensile tests on the TPU were performed at a constant test speed of 50 mm/min, continuing until the strain reached 400%. To examine potential aniso-tropy in the material's behaviour, two groups of test specimens were prepared with different orientations Group 1: Specimens were constructed with their main axes aligned in the same direction. Group 2: Specimens were built with their main axes also parallel to each other but perpendicular to those in Group 1. Tensile tests were carried out on both sets, and the average mechanical behaviour for both perpendicular directions of the material is shown in the graphs in Figure 10a.

The results reveal that the TPU can achieve significant strain levels of up to 400% before failure. Additionally, a minimal difference is seen in the mechanical responses between the specimens, implying that the TPU has a nearly isotropic behaviour at the 50 mm/min test speed. For lower test speeds like 5 and 10 mm/min that require a longer testing duration, a stopping cri-terion was applied. Tests were automatically terminated once the specimens reached a 200% strain level that is adequate and practical for many engineering
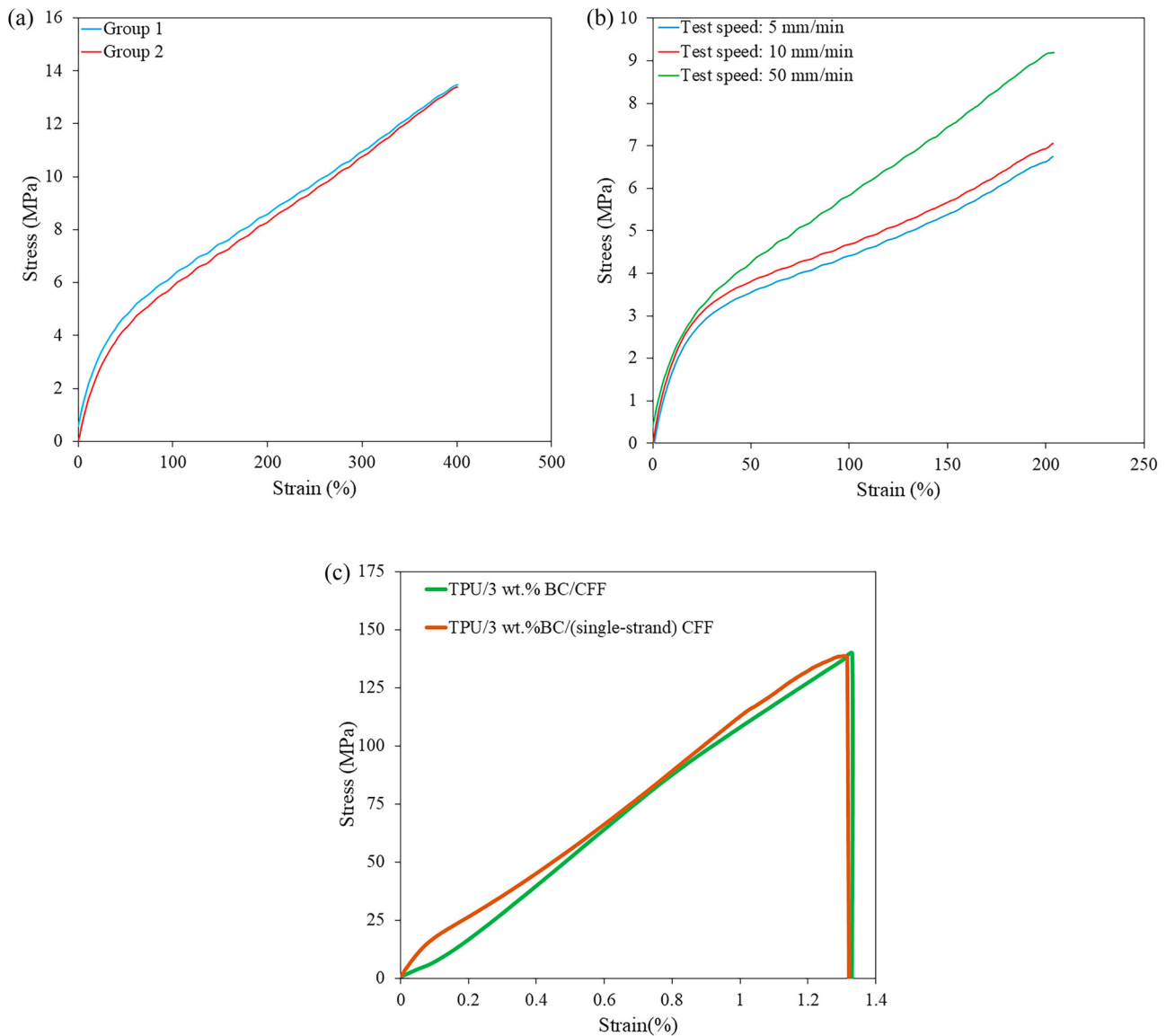
Figure 10. (a) The stress-strain results of the monotonic tensile test to study potential anisotropy on two groups (axes parallel and axes perpendicular) of the TPU tested at 50 mm/min, (b) the stress-strain results of monotonic tensile test of the pure TPU tested at different speeds (c) a comparison of the stress–strain behaviour at 50 mm/min between a single CFF embedded in a TPU/3 wt.% BC matrix and the full TPU/3 wt.% BC/CFF composite.

applications [42]. The slowest speed, i.e. 5 mm/min, was regarded as representative of the quasi-static condition. Figure 10b depicts the results of monotonic tensile tests on the TPU with various speeds. It can be found that increasing the testing speed (~strain rate) hardens the material in terms of the mechanical response [18]. The maximum tensile stress of the specimens increases as the strain rate is increased. These phenomena are due to higher strain rates shifting the behaviour of the TPU specimens from ductile to brittle, making the slope in the linear elastic region followed by hyper-elastic strain softening steeper.

Figure 10c presents a comparison of the stress–strain behaviour between a single CFF embedded in a TPU/3 wt.% BC matrix and the full TPU/3 wt.% BC/CFF composite. The single CFF in TPU/BC matrix sample was printed using the same modified FFF 3D printing setup (Original Prusa MINI+, 1.8 mm nozzle, 235 °C) as the full composite samples. However, in this case, a single layer was designed in SolidWorks and sliced in Prusa Slicer. During printing, the CFF was fed through one channel of the extruder, and the TPU/3 wt.% BC filament was fed through the other. As a result, one layer of TPU/BC matrix with a single embedded CFF was printed. The figure reveals a minimal difference in the mechanical responses between the specimens. This difference can be attributed to the probability of void formation within the matrix of the full sample, and particularly at the fibre–matrix interface. It becomes more pronounced due to incomplete impregnation and limited polymer flow, especially around natural fibres.

The counterpart of Figure 10 for TPU with various BC contents and CFF is presented in Figure 11. Comparing the results in Figure 11 proves that increasing the testing speed or strain rate always hardens the TPU with and without particle and reinforcements and makes the material stiffer. Particularly, TPU/BC reinforced with CFF experiences reduced ductility and increased brittleness. Furthermore, it is seen that both pure TPU and TPU/BC have a non-linear hyper-elastic behaviour implying that the BC particle reinforcement does not affect the mechanical behaviour trend. On the other hand, however, it is found that the continuous fibre reinforcement affects the mechanical response, and the composite behaves almost linearly before a sudden breakage. Next, Figure 11a reveals that the highest tensile strength is achieved in samples containing 3% by weight of BC (TPU/3 wt.% BC) compared to the pure TPU (7.06 MPa) without CFF at 200% strain level. However, further increasing the BC content (e.g. TPU/5 wt.% BC) results in a decline in tensile strength and stiffness. This drop in the mechanical property could have two possible reasons: (1) Excessive BC

particles may compromise filament uniformity, causing issues during the printing process and preventing the production of high-quality samples [43]. (2) The aggregation of BC particles and the formation of clusters within the TPU matrix could create micro-voids between the particles and the polymer, disrupting stress transfer when the tensile force is applied [44]. These reasons, including excessive BC particles and aggregation of BC particles, are consistent with the microstructural features observed in the SEM images presented in Figure 5 (Section 3.1), where clear signs of micro-voids. Figure 11b shows among the tested samples at the speed of 5 mm/min, TPU/3 wt.% BC/CFF experiences the highest strength of 118 MPa. This performance exceeds that of TPU/0 wt.% BC/CFF, TPU/5 wt.% BC/CFF, and TPU/3 wt.% BC. The tensile strength of TPU/3 wt.% BC/CFF is approximately 37% 78%, 1278% and 1571% greater than that of TPU/5 wt.% BC/CFF, TPU/0 wt.% BC/CFF, TPU/3 wt.% BC and TPU, respectively. The 1571% improvement compared to pure TPU (7.06 MPa at 200% strain) is calculated as follows:

$$\frac{118\,MPa(TPU/3\,wt.\%\,BC/CFF)_{max} - 7.06\,MPa(Pure\,TPU)_{200\%\,Strian}}{7.06\,MPa(Pure\,TPU)_{200\%\,Strian}}$$
$$\times 100\% = 1571\%$$

The observed increase in tensile strength of TPU/3 wt.% BC /CFF composites can be attributed to two primary factors: (1) Effective load transfer at the fibre-matrix interface and the inherent ductility of the CFF [34]. The strong interfacial bonding between the flax fibres and the TPU/BC matrix ensures efficient stress distribution, preventing premature failure and enhancing overall mechanical performance. (2) The ductility of the CFF allows for greater energy absorption and delayed crack propagation, further contributing to the improved tensile strength of the composite [34]. These combined effects result in a stronger and durable composite capable of withstanding higher tensile loads.

3.5.2. Cyclic tensile tests

To evaluate the Mullins effect, stress reduction due to hysteresis and damage, and strain sensitivity, uniaxial tensile cyclic tests were conducted on the TPU and TPU/BC bio-composites at strain levels of 50, 100, and 150%. For each strain level, one and three load-unload cycles were performed. At the end of each unloading phase (i.e. when the force reaches zero), the strain did not return to zero, primarily due to the viscous nature of the material, lacking sufficient time to fully recover the original state. Therefore, to avoid buckling, the specimens were unloaded to a strain corresponding to a small tensile force of 0.1 N. The testing procedure began with
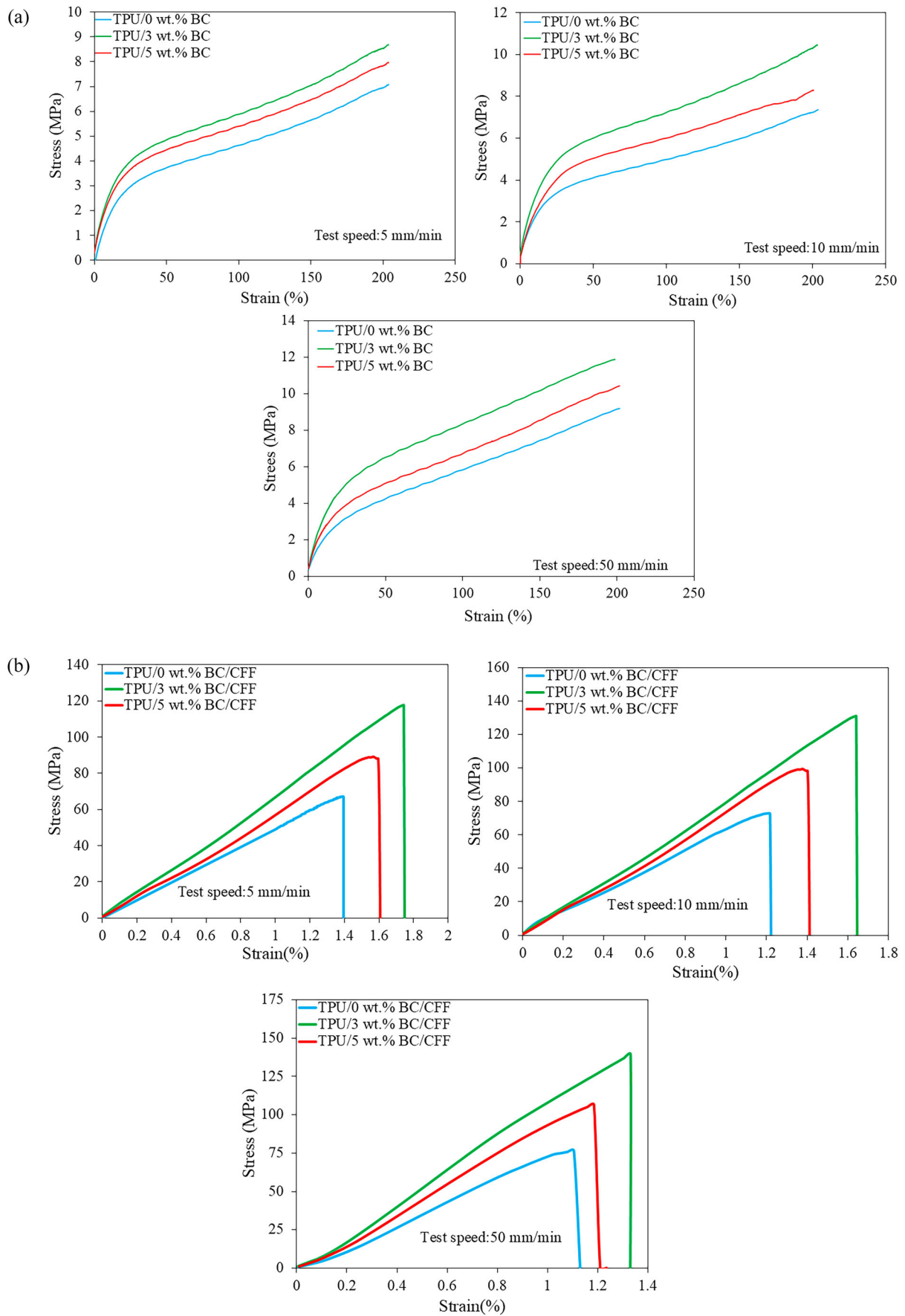
Figure 11. The stress-strain results of monotonic tensile test of (a) TPU/BC and (b) TPU/BC/CFF bio-composites at different speeds.

an initial preload of 0.1 N, followed by three load-unload cycles up to 50% engineering strain. This was repeated for three cycles up to 100% strain and finally three cycles up to 150% strain. The choice of three cycles was made to assess the material's response to low-cycle fatigue, permanent residual deformation, and its combined hyper-visco-pseudo-elastic (HVPE) behaviours under repeated loading [45]. Engineering stresses and strains were calculated by normalising the measured force and displacement values by the initial (unde-formed) cross-sectional area and length of the speci-mens. Figures 12a–d present cyclic stress–strain response and strain time history of 3D-printed TPU bio-composites reinforced with 0, 3, and 5 wt.% BC and CFF, and tested at 5 mm/min speed. Furthermore, Figure 13 shows a detailed cyclic stress–strain behaviour of TPU/3 wt.% BC bio-composite under loading, unload-ing, and re-loading for three cycles.

It can be found from Figures 12 and 13 that the loading and unloading curves do not coincide, instead exhibiting HVPE behaviour. At any given strain after unloading, the stress level during reloading is also lower than the stress needed to achieve the same strain during loading. It shows a significant change in the hyper-elastic behaviour and is attributed to an increase in stress concentration sites and slipping locations along the filler material. This phenomenon is referred to as HVPE, the Mullins effect, or stress softening and is caused by the microstructural damage of the solid occurring mainly during the initial loadings [17]. Further-more, non-zero strains corresponding to the zero-stress state may be residual strains resulting from the Mullins effect combined with hysteretic/visco-elastic behaviour and a permanent plastic deformation. The results imply that the TPU and TPU bio-composites have a HVPE behaviour during large cyclic loadings.

Figure 13 illustrates hysteresis loops during repeated loading-unloading cycles. The hysteresis loops represent the energy absorbed and dissipated due to the material's HVPE properties. The gradual reduction in elastic modulus and the increase in residual strain after each cycle are attributed to the Mullins effect, indicating structural damage and a decrease in stiffness. Also, with variations in loop width and position, their mechanical properties and energy dissipation capabilities differ. At higher strain levels, the non-linear behaviour demon-strates the material's hyper-elastic properties, while the reversible strain recovery with time dependence is attributed to the combined pseudo-elastic and visco-elastic nature of the material. This analysis is particularly relevant for applications that demand resistance to cyclic loading, energy absorption, or the ability to with-stand significant deformations without breakage. The

hysteresis loops observed in Figure 13 and the area within each loop represent the energy absorbed and dis-sipated per cycle. TPU/3 wt.% BC exhibits wider loops compared to TPU/0 wt.% BC and TPU/5 wt.% BC, indicat-ing a higher energy dissipation capacity. This suggests that TPU/3 wt.% BC is more effective at absorbing and dissipating energy under cyclic loading. This feature makes the bio-composite potentially more suitable for applications requiring enhanced damping or shock absorption properties. The progressive shift of the loops to the right with increasing strain further high-lights the materials' visco-elastic behaviour under repeated loading conditions.

4. Meta-bio-composite structures

Advances in multi-material composite 3D printing are enabling the development of high-performance engin-eering structures that benefit from both material and structural synergies [46]. Cellular lattice structures, such as meta-material honeycombs, possess high specific strength and stiffness and provide a high energy-absorption-to-weight ratio [47]. Lattice structures could benefit from multi-material design and manufacturing strategies to enhance their mechanical performance. In this research, the pure TPU and TPU reinforced by BC and CFF with inherent energy absorption and dissipa-tion were 3D printed to create honeycomb meta-struc-tures with supreme energy absorption/dissipation, which originated from both parent material and geo-metrical properties.

Bio-composite meta-materials featuring a hexagonal cross-section were designed and 3D printed with and without BC and CFF reinforcements, as depicted in Figure 14a. They were tested via an in-plane com-pression loading and unloading at a rate of 5 mm/min, reaching a maximum global strain level of 50% (of the original height = 35 mm). Immediately after unloading, the sample height was measured. Their configuration during loading-unloading steps is displayed in Figures 14b–d. However, the samples gradually recovered to their original shape within one hour. The force-displace-ment response curves during loading and unloading are also presented in Figure 14e. The samples recover immediately upon the removal of the force, potentially releasing all hyper-visco-elastic deformations The results in Figures 14b indicate that the meta-bio-compo-site TPU and TPU reinforced with various BC contents can release all hyper-visco-elastic deformations and fully recover their original shape/height after being com-pressed to 50% axial global strain and unloading. In con-trast, the TPU/BC bio-composite reinforced with CFF shows a residual irrecoverable inelastic deformation
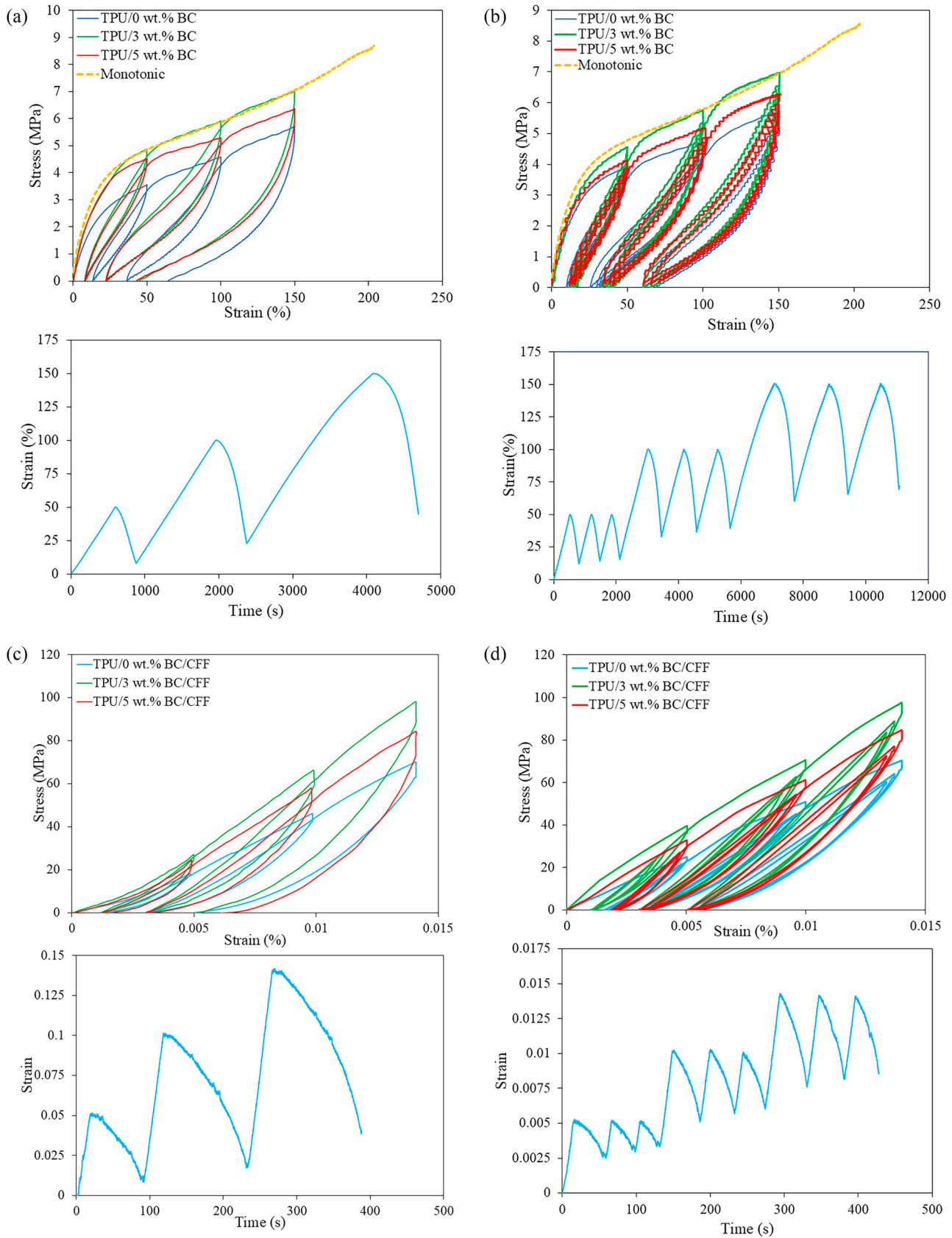
Figure 12. The stress-strain response and strain time history of 3D-printed TPU-based bio-composites reinforced with 0, 3, and 5 wt.% BC (a, b) and CFF (c, d) under three loading-unloading cycles with (a, c) and without (b, d) repetition.
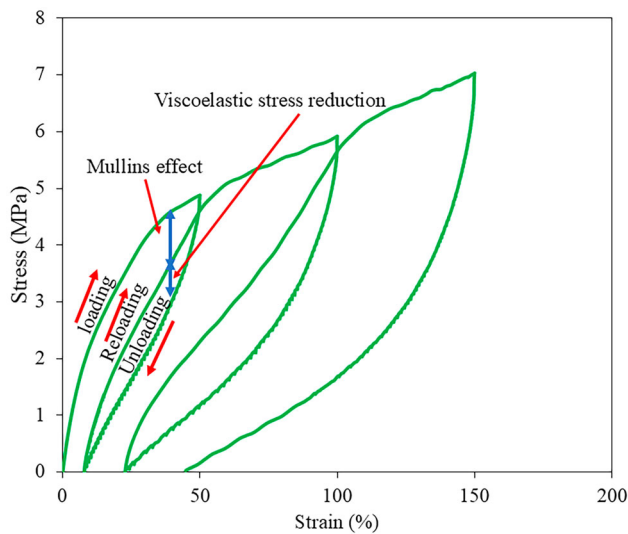
Figure 13. The cyclic stress-strain response of TPU/3 wt.% BC bio-composite under loading, unloading, and re-loading.

after loading to achieve 50% global strain and fully unlading followed by a recovery phase, see Figures 14c–e. TPU/BC/CFF meta-bio-composite can partially recover its original deformation/height while %10 global strain or 3.5 mm height reduction remains in the structures after fully unloading and a recovery phase. The residual irrecoverable deformation could be associated with the inelastic deformation in the CFF and local damage to the fibres at micro and macro scales. To investigate this residual deformation, Figure 14e shows SEM images with different magnifications from the cross-section of a representative meta-bio-composite sample (TPU/3 wt.% BC/CFF) before and after loading. SEM original images are provided in the supplementary material (Figure S5) to support this observation. As illustrated in the microstructure, no significant damage or structural changes were observed. This can be attributed to the hyper-elastic behaviour of the TPU matrix, which allows the structure to return nearly to its original configuration after deformation.

A key conclusion from Figure 14e is that reinforcement in the form of particles and/or fibres can significantly influence the mechanical behaviour of meta-structures. The analysis reveals that pure TPU exhibits hyper-elastic behaviour with a linear loading response, whereas the addition of BC particles stiffens the meta-structure. This stiffening effect leads to: (1) an increased slope in the force-displacement loading curve (greater stiffness), (2) an expanded hysteresis area, and (3) an enhanced maximum force. Notably, the incorporation of CFF into TPU and TPU/BC not only further stiffens the meta-structure and significantly improves energy absorption/dissipation capacity but also substantially

alters its mechanical behaviour. Furthermore, the TPU/BC/CFF meta-bio-composites demonstrate superior force regulation compared to TPU and TPU/BC, which exhibit an almost linear mechanical response during loading. While TPU and TPU/BC display positive stiffness, the addition of CFF introduces a quasi-plateau response. In this state, the structure exhibits a quasi-zero stiffness, maintaining a nearly constant force over a specific deformation range – for example, 12 mm for TPU/3 wt.% BC/CFF. This unique behaviour reduces peak forces and stresses, enhances energy dissipation, prevents excessive load buildup, and provides stress relief. Such controlled regulation of force and stiffness is particularly advantageous for applications involving impact mitigation, vibration isolation, overload protection, and pressure adaptation. The overload protection feature could also be useful in human interactions and enhance comfort. These properties make flexible TPU/BC/CFF composites highly durable and well-suited for protective, ergonomic, and safety-focused applications.

Next, the mechanical behaviour of meta-bio-composites is evaluated, focusing on their energy absorption and dissipation capabilities. In cyclic loading analysis, the absorbed and dissipated energies of visco-elastic or hyper-elastic materials can be evaluated using stress–strain hysteresis loops. During each loading–unloading cycle, internal friction and nonlinear deformation result in a loop-shaped curve. The absorbed energy corresponds to the area under the loading curve and represents the total mechanical work input into the material. In contrast, the dissipated energy is given by the area enclosed within the hysteresis loop, which reflects the energy lost due to internal damping and irreversible deformation. The stored or recoverable energy is represented by the area under the unloading curve and accounts for the elastic portion of the deformation. While stress–strain hysteresis loops are recognised for material-level energy analysis [48,49], it is important to note that force–displacement curves are also a well-established and validated method for calculating absorbed or dissipated energy, particularly in structural-scale evaluations of cellular and meta-materials [50–52]. In this study, the energy values were determined by calculating the area enclosed within the loading–unloading force–displacement curves, an approach extensively used in the literature for assessing energy absorption under compressive loading. Foundational works by Johnson and Mamalis [53] and Jones [51] provide both theoretical and experimental support for using force–displacement data in crashworthiness and impact energy analyses. Zhang et al. [54] also investigated the energy absorption behaviour of multi-cell
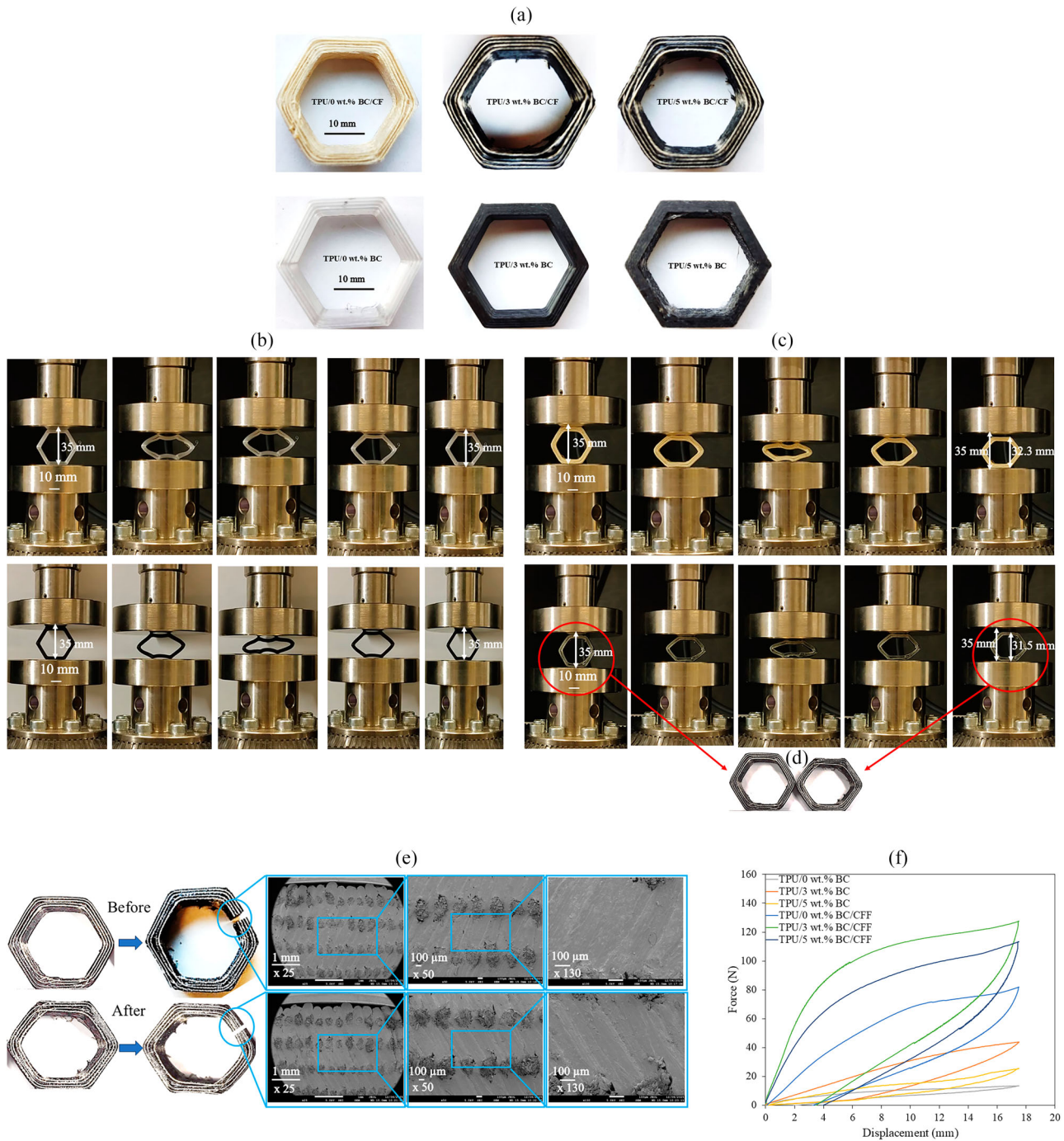
Figure 14. 3D printed meta-bio-composites with a hexagonal cross-section (a); configuration of the TPU, TPU/3 wt.% BC (b) and TPU/0 wt.% BC/CF, and TPU/3 wt.% BC/CFF (c) during loading up to 50% compression and uploading followed by a recovery phase; configuration of the TPU/3 wt.% BC/CFF meta-bio-composite before and after loading showing an irrecoverable deformation (d); images of residual deformation SEM with different magnifications from the cross-section of a representative meta-bio-composite sample (TPU/3 wt.% BC/CFF) before and after loading (e); the force-displacement response of various meta-bio-composites under a loading-unloading-recovery cycle (f).

thin-walled columns under axial compression. They demonstrated that the absorbed energy can be accurately estimated by calculating the area under the force–displacement curve, using both theoretical models and finite element simulations The yellow and green areas under the loading and unloading curves represent energy dissipation and absorption, respectively. These energy components help assess the material's damping capacity, energy absorption potential, and fatigue behaviour. They can be estimated
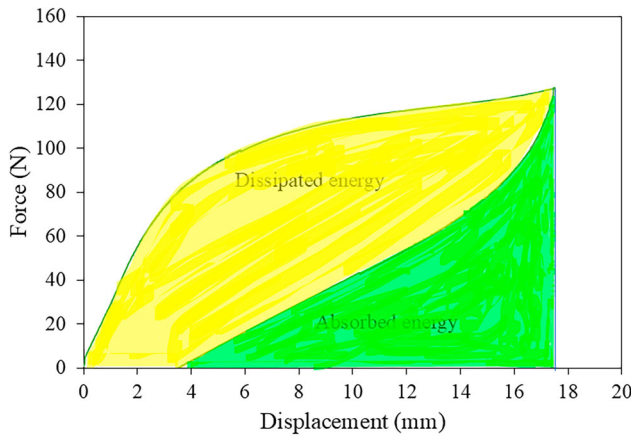
Figure 15. The force-displacement response of TPU/3 wt.% BC/CFF meta-bio-composite highlighting dissipated and absorbed energies.

numerically via integration methods from experimental plots (see Figure 14). Figure 15 depicts the energy absorbed and dissipated by the TPU/3 wt.% BC/CFF meta-bio-composite under 50% global strain. Additionally, the specific energy absorption (SEA) for all meta-structures was calculated and is presented in Figure 16. For a comprehensive explanation of the SEA calculation, one may refer to [34].

The results indicate that the meta-bio-composite can effectively dissipate a significant amount of kinetic energy. It is observed that adding simultaneously 3 wt.% BC and CFF to TPU and CFF to TPU enhances the SEA of TPU by 933% and 866%, respectively. The synergistic combination of these two reinforcements in TPU

leads to a maximum SEA of 31 J/g, marking a 933% improvement compared to pure TPU (3 J/g). The percentage improvement is calculated as follows:

$$\frac{31(\mathit{TPU/3wt.\%BC/CFF})_{SEA} - 3(\mathit{Pure\ TPU})_{SEA}}{3(\mathit{TPU})_{SEA}} \times 100\%$$

$$= 933\%$$

These findings contribute to the creation of a comprehensive library of bio-composite materials, providing a systematic understanding of how material composition impacts mechanical performance within a single meta-structure geometry. This framework serves as a valuable tool for designers in selecting optimal material-geometry combinations for specific applications, particularly those requiring both mechanical strength and flame resistance.

The strength-to-weight ratio, a key indicator for lightweight structural efficiency, exhibits an improvement with the addition of both BC and CFF reinforcements. As shown in Figure 16 and Table 5, the addition of BC enhanced the ratio, and the incorporation of CFF leads to a significant increase in performance, particularly in the TPU/3 wt.% BC/CFF sample, achieving the maximum strength-to-weight ratio of 700% compared to pure TPU. This enhancement reflects the synergistic effect of particle and fibre reinforcement, where CFF contributes to improved load transfer and structural integrity without adding excessive mass. Notably, even at 5 wt.% BC with CFF, the ratio remains considerably higher than that of the neat TPU, confirming the effectiveness of bio-based reinforcements for applications
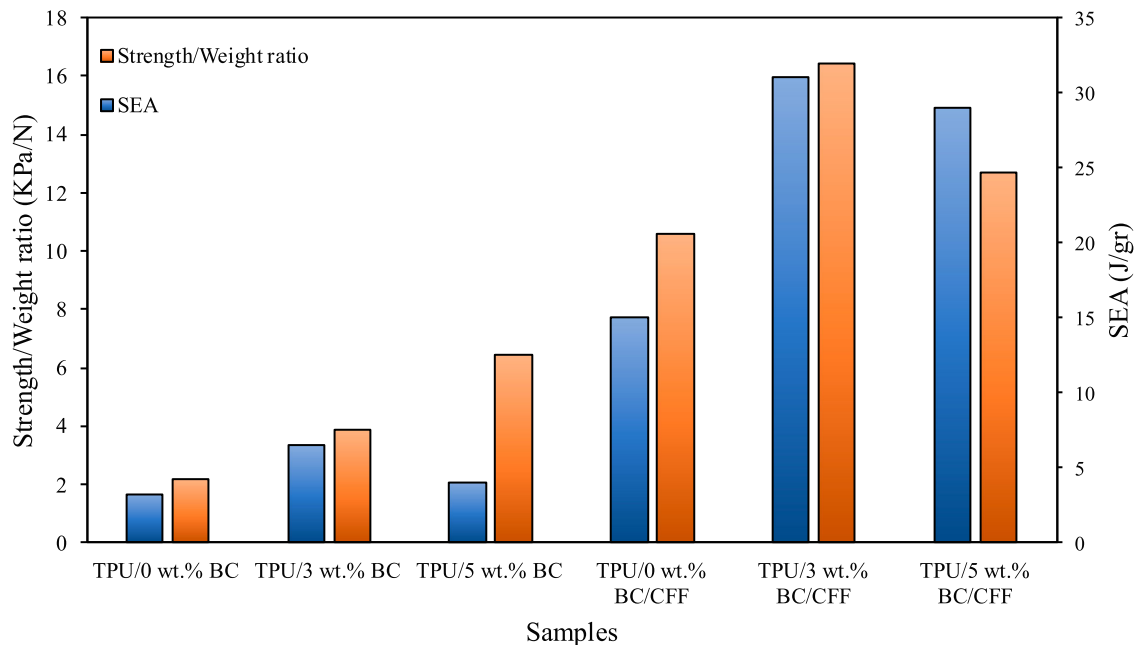

Figure 16. The SEA values calculated for all meta-structures.

Table 5. Strength-Weight ratio for specimens the TPU/BC bio-composites.

Samples	Strength (KPa)	Weight (N)	Strength to weight ratio (KPa/N)
TPU/0 wt.% BC	67	31	2
TPU/3 wt.% BC	127	32.5	4
TPU/5 wt.% BC	217	33.7	6
TPU/0 wt.% BC/CFF	409	38.4	11
TPU/3 wt.% BC/CFF	638	39.8	16
TPU/5 wt.% BC/CFF	567	42.6	13

where mechanical strength and lightweight design are simultaneously critical.

5. Conclusion

The demand for high-performance, sustainable materials has driven the development of bio-composites that balance mechanical strength, flame retardancy, and energy absorption/dissipation. This study pioneers a TPU-based bio-composite reinforced with bamboo charcoal and continuous flax fibres, demonstrating exceptional thermo-mechanical performance, processability, and environmental benefits. The key findings and contributions are summarised as follows:

Microstructural analysis using SEM imaging confirmed strong fibre-matrix adhesion, reducing defects and enhancing stress transfer. The incorporation of 3 wt.% BC and CFF led to a significant 1571% increase in tensile strength compared to pure TPU, while flame retardancy was also greatly enhanced, as evidenced by a 52% reduction in burning rate, attainment of a UL-94 V-1 rating, and a LOI of 29.5 vol.%. Low-fatigue cyclic tests revealed HVPE behaviour, the Mullins effect and stress softening, indicating the material's suitability for cyclic and impact-related energy-dissipation applications. The melt flow index analysis confirmed that the composite retained its extrudability and 3D printability, enabling effective filament production and 3D printing. Moreover, the quasi-zero stiffness meta-bio-composites demonstrated force regulation and impact resistance features with a 933% increase in specific energy absorption over pure TPU. They highlight their potential for energy absorption/dissipation and protective applications. The environmentally friendly, lightweight nature of the bio-based composition aligns with circular economy principles, offering a viable alternative to synthetic composites. These TPU/BC/CFF bio-composites and their meta-structures present a transformative material/structural element solution for automotive, transportation, construction, furniture, and medical/sport/safety gear applications, bridging eco-conscious innovation with superior functional performance.

Disclosure statement

The authors declare that they have no known competing financial interests or personal relationships that could have appeared to influence the work reported in this paper.

Author contributions

CRediT: **Kaveh Rahmani:** Data curation, Formal analysis, Investigation, Methodology, Validation, Visualization, Writing – original draft, Writing – review & editing; **Callum Branfoot:** Investigation, Methodology, Supervision, Writing – review & editing; **Sarah Karmel:** Investigation, Methodology, Supervision, Writing – review & editing; **Kevin Lindsey:** Investigation, Methodology, Writing – review & editing; **Mahdi Bodaghi:** Conceptualization, Funding acquisition, Investigation, Methodology, Project administration, Resources, Supervision, Validation, Writing – original draft, Writing – review & editing.

Data availability statement

The data that support the findings of this study are available in Zenodo at https://doi.org/10.5281/zenodo.15490464.

ORCID

Mahdi Bodaghi http://orcid.org/0000-0002-0707-944X

References

[1] Goh GD, Yap YL, Agarwala S, et al. Recent progress in additive manufacturing of fiber reinforced polymer

composite. Adv Mater Technol. 2019;4(1):1800271. doi:10.1002/admt.201800271

[2] Parandoush P, Lin D. A review on additive manufacturing of polymer-fiber composites. Compos Struct. 2017;182:36–53. doi:10.1016/j.compstruct.2017.08.088

[3] Van Der Klift F, Koga Y, Todoroki A, et al. 3D printing of continuous carbon fibre reinforced thermo-plastic (CFRTP) tensile test specimens. Open J Compos Mater. 2015;6(1):18–27. doi:10.4236/ojcm.2016.61003

[4] Mei H, Ali Z, Ali I, et al. Tailoring strength and modulus by 3D printing different continuous fibers and filled structures into composites. Adv Compos Hybrid Mater. 2019;2:312–319. doi:10.1007/s42114-019-00087-7

[5] Moshood TD, Nawanir G, Mahmud F, et al. Biodegradable plastic applications towards sustainability: a recent innovations in the green product. Cleaner Eng Technol. 2022;6:100404. doi:10.1016/j.clet.2022.100404

[6] Andanje MN, Mwangi JW, Mose BR, et al. Biocompatible and biodegradable 3D printing from bioplastics: A review. Polymers (Basel). 2023;15(10):2355. doi:10.3390/polym15102355

[7] Andanje M, Mwangi J, Mose B, et al. Biocompatible and biodegradable 3D printing from bioplastics: a review. Polymers (Basel). 2023;15:2355. doi:10.3390/polym15102355

[8] Li M, Pu Y, Thomas VM, et al. Recent advancements of plant-based natural fiber – reinforced composites and their applications. Compos B Eng. 2020;200:108254. doi:10.1016/j.compositesb.2020.108254

[9] Fortea-Verdejo M, Bumbaris E, Burgstaller C, et al. Plant fibre-reinforced polymers: where do we stand in terms of tensile properties? Int Mater Rev. 2017;62(8):441–464. doi:10.1080/09506608.2016.1271089

[10] Ahmed W, Alnajjar F, Zaneldin E, et al. Implementing FDM 3D printing strategies using natural fibers to produce biomass composite. Materials (Basel). 2020;13(18):4065. doi:10.3390/ma13184065

[11] Zhang H, Liu D, Huang T, et al. Three-dimensional printing of continuous flax fiber-reinforced thermoplastic composites by five-axis machine. Materials (Basel). 2020;13(7):1678. doi:10.3390/ma13071678

[12] Turjo SKS, Hossain MF, Rana MS, et al. Mechanical characterization and corrosive impacts of natural fiber reinforced composites: an experimental and numerical approach. Polym Test. 2023;125:108108. doi:10.1016/j.polymertesting.2023.108108

[13] Fan Q, Duan H, Xing X. A review of composite materials for enhancing support, flexibility and strength in exercise. Alexandria Eng J. 2024;94:90–103. doi:10.1016/j.aej.2024.03.048

[14] Tian X, Todoroki A, Liu T, et al. 3D printing of continuous fiber reinforced polymer composites: development, application, and prospective. Chinese J Mech Eng: Addit Manuf Front. 2022;1(1):100016. doi:10.1016/j.cjmeam.2022.100016

[15] Case JC, White EL, Kramer RK. Soft material characterization for robotic applications. Soft Robotics. 2015;2(2):80–87. doi:10.1089/soro.2015.0002

[16] Cantournet S, Desmorat R, Besson J. Mullins effect and cyclic stress softening of filled elastomers by internal sliding and friction thermodynamics model. Int J Solids Struct. 2009;46(11-12):2255–2264. doi:10.1016/j.ijsolstr.2008.12.025

[17] Fazekas B, Goda TJ. Constitutive modelling of rubbers: Mullins effect, residual strain, time-temperature dependence. Int J Mech Sci. 2021;210:106735, doi:10.1016/j.ijmecsci.2021.106735

[18] bin Che'Harun MF, Ghani M. The effects of strain rates on the mechanical properties of thermoplastic polyurethane. J Mater Sci. 2021;2(1):54–63.

[19] Pechlivani EM. 3D printing TPU composites infused with continuous carbon fibers for impact absorption applications. Int J Modern Manuf Technol XVI. 2024;3:40–46. doi:10.54684/ijmmt.2024.16.3.40

[20] Hao M, Wang J, Wang R, et al. Mechanical dependence of 3D-printed thermoplastic polyurethane reinforced with minor continuous carbon fibres. Virtual Phys Prototyp. 2023;18:e2224304, doi:10.1080/17452759.2023.2224304

[21] Woigk W, Fuentes C, Rion J, et al. Interface properties and their effect on the mechanical performance of flax fibre thermoplastic composites. Compos Part A Appl Sci Manuf. 2019;122:8–17. doi:10.1016/j.compositesa.2019.04.015

[22] Tayfun U, Dogan M, Bayramli E. Investigations of the flax fiber/thermoplastic polyurethane eco-composites: influence of isocyanate modification of flax fiber surface. Polym Compos. 2017;38(12):2874–2880. doi:10.1002/pc.23889

[23] Tayfun U, Dogan M, Bayramli E. Influence of surface modifications of flax fiber on mechanical and flow properties of thermoplastic polyurethane based eco-composites. J Nat Fibres. 2016;13(3):309–320. doi:10.1080/15440478.2015.1029191

[24] Ansaripour A, Heidari-Rarani M. Hybrid toughening effect of flax fiber and thermoplastic polyurethane elastomer in 3D-printed polylactic acid composites. Polym Compos. 2024;45(18):17239–17256. doi:10.1002/pc.28965

[25] Sabet M. Advancements in halogen-free polymers: exploring flame retardancy, mechanical properties, sustainability, and applications. Polymer-Plastics Technol Mater. 2024;63(13):1794–1818. doi:10.1080/25740881.2024.2359633

[26] Liu BW, Zhao HB, Wang YZ. Advanced flame-retardant methods for polymeric materials. Adv Mater. 2022;34(46):2107905. doi:10.1002/adma.202107905

[27] Prasad V, Alliyankal Vijayakumar A, Jose T, et al. A comprehensive review of sustainability in natural-fiber-reinforced polymers. Sustainability. 2024;16(3):1223. doi:10.3390/su16031223

[28] Ahmad MN, Ishak MR, Mohammad Taha M, et al. A review of natural fiber-based filaments for 3D printing: filament fabrication and characterization. Materials (Basel). 2023;16(11):4052. doi:10.3390/ma16114052

[29] Wu Q, Liu Y, Han Z, et al. Surface modification of bamboo fibers by diammonium phosphate and their applications in flame retardant thermoplastic polyurethane. J Appl Polym Sci. 2021;138(25):50606. doi:10.1002/app.50606

[30] Atabek Savas L, Mutlu A, Dike AS, et al. Effect of carbon fiber amount and length on flame retardant and mechanical properties of intumescent polypropylene composites. J Compos Mater. 2018;52(4):519–530. doi:10.1177/0021998317710319

[31] Zhang C, Shi M, Zhang Y. EG/TPU composites with enhanced flame retardancy and mechanical properties prepared by microlayer coextrusion technology. RSC Adv. 2019;9:23944–23956. doi:10.1039/C9RA03653A

[32] Alhanish A, Abu Ghalia M. Biobased thermoplastic polyurethanes and their capability to biodegradation. In: Eco-friendly adhesives for wood and natural fiber composites: characterization, fabrication and applications. 2021. p. 85–104. doi:10.1007/978-981-33-4749-6_4

[33] Rochman A, Delia S. (2024). Additive manufacturing of thermoplastic polyurethane elastomers: a review.

[34] Bodaghi M, Rahmani K, Dezaki ML, et al. 3D/4D printed bio-composites reinforced by bamboo charcoal and continuous flax fibres for superior mechanical strength, flame retardancy and recoverability. Polym Test. 2025;143: 108709, doi:10.1016/j.polymertesting.2025.108709

[35] Wang Y, Li Z, Li X, et al. Effect of the temperature and strain rate on the tension response of uncured rubber: experiments and modeling. Mech Mater. 2020;148: 103480, doi:10.1016/j.mechmat.2020.103480

[36] Chenrayan V, Shahapurkar K, Kanaginahal GM, et al. Evaluation of dynamic mechanical analysis of crump rubber epoxy composites: experimental and empirical perspective. J Brazilian Soc Mech Sci Eng. 2023;45(3): 145, doi:10.1007/s40430-023-04033-z

[37] Zhang S, Hu W, He H, et al. Simultaneously strengthening, toughening, and damage monitoring of fiber reinforced composite by using a rigid/flexible hybrid modifier. Polym Compos. 2025;46(4):3009–3029. doi:10. 1002/pc.29150

[38] Sethi S, Ray BC. Environmental effects on fibre reinforced polymeric composites: evolving reasons and remarks on interfacial strength and stability. Adv Colloid Interface Sci. 2015;217:43–67. doi:10.1016/j.cis.2014.12.005

[39] Chenrayan V, Kanaginahal G, Shahapurkar K, et al. Analytical modeling and experimental estimation of the dynamic mechanical characteristics of green composite: Caesalpinia decapetala seed reinforcement. Polymer Eng Sci. 2024;64(3):1096–1109. doi:10.1002/ pen.26599

[40] Shenavar A, Abbasi F, Aghjeh MR, et al. Flow and mechanical properties of carbon black filled acrylonitrile-butadiene-styrene (ABS). J Thermoplast Compos Mater. 2009;22(6):753–766. doi:10.1177/0892705709103225

[41] Kanaginahal GM, Tambrallimath V, Murthy M, et al. Flammability studies of natural fiber-reinforced polymer composites fabricated by additive manufacturing technology: a review. J Inst Eng: Series D. 2024;105(2):1291–1303. doi:10.1007/s40033-023-00509-3

[42] Melly SK, Liu L, Liu Y, et al. A review on material models for isotropic hyperelasticity. Int J Mech Syst Dynam. 2021;1(1):71–88. doi:10.1002/msd2.12013

[43] Kantaros A, Drosos C, Papoutsidakis M, et al. Composite filament materials for 3D-printed drone parts: advancements in mechanical strength, weight optimization and embedded electronics. Mater. 2025;18(11):2465. doi:10. 3390/ma18112465

[44] Mehdikhani M, Gorbatikh L, Verpoest I, et al. Voids in fiber-reinforced polymer composites: A review on their formation, characteristics, and effects on mechanical performance. J Compos Mater. 2019;53(12):1579–1669. doi:10.1177/0021998318772152

[45] Fazekas B, Goda TJ. New numerical stress solutions to calibrate hyper-visco-pseudo-elastic material models effectively. Mater Des. 2020;194:108861. doi:10.1016/j. matdes.2020.108861

[46] Alarifi IM. Revolutionising fabrication advances and applications of 3D printing with composite materials: a review. Virtual Phys Prototyp. 2024;19(1):e2390504. doi:10.1080/ 17452759.2024.2390504

[47] Bodaghi M, Van Hoa S, Gries T, et al. Focus on 4D materials design and additive manufacturing. Smart Mater Struct. 2023;32(110401):4.

[48] Avalle M, Belingardi G, Montanini R. Characterization of polymeric structural foams under compressive impact loading by means of energy-absorption diagram. Int J Impact Eng. 2001;25(5):455–472. doi:10.1016/S0734-743X(00)00060-9

[49] Avalle M. A generic model to assess the efficiency analysis of cellular foams. Materials (Basel). 2024;17(3):746. doi:10. 3390/ma17030746

[50] Wierzbicki T, Abramowicz W. (1983). On the crushing mechanics of thin-walled structures.

[51] Jones N. Structural impact. Cambridge: Cambridge University Press 1989; 1997.

[52] Jones N. (1989). Recent studies on the dynamic plastic behavior of structures.

[53] Mamalis AG, Manolakos D, Demosthenous G, et al. Crashworthiness of composite thin-walled structures. Lancaster, PA: CRC Press; 2017.

[54] Zhang X, Cheng G, Zhang H. Theoretical prediction and numerical simulation of multi-cell square thin-walled structures. Thin-Walled Struct. 2006;44(11):1185–1191. doi:10.1016/j.tws.2006.09.002